

Milestones in X-ray microscopy:
Scanning X-ray microscopy,
spectromicroscopy and
recent achievements

Janos Kirz
ALS &
Stony Brook University

Outline

- 1/ History - as I see it
 - Comments on X-ray microprobes
- 2/ STXM at the ALS, NSLS and elsewhere
- 3/ Variations: SPEM, SLXM, SXRF
- 4/ Conclusions
 - where different forms of x-ray microscopy fit in.

H. H. Pattee Jr.
The Scanning X-ray Microscope
JOSA 43, 61 (1953)

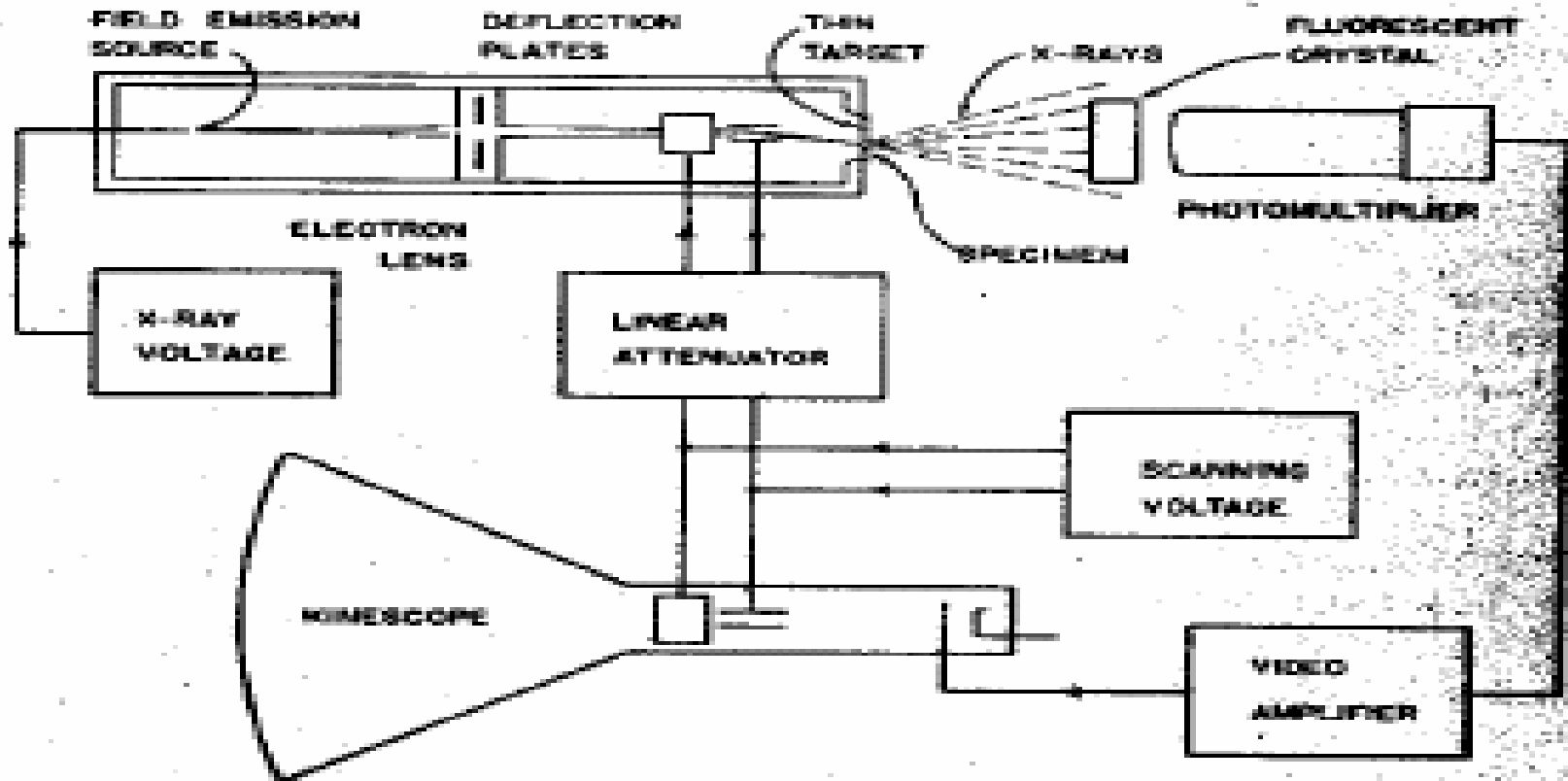
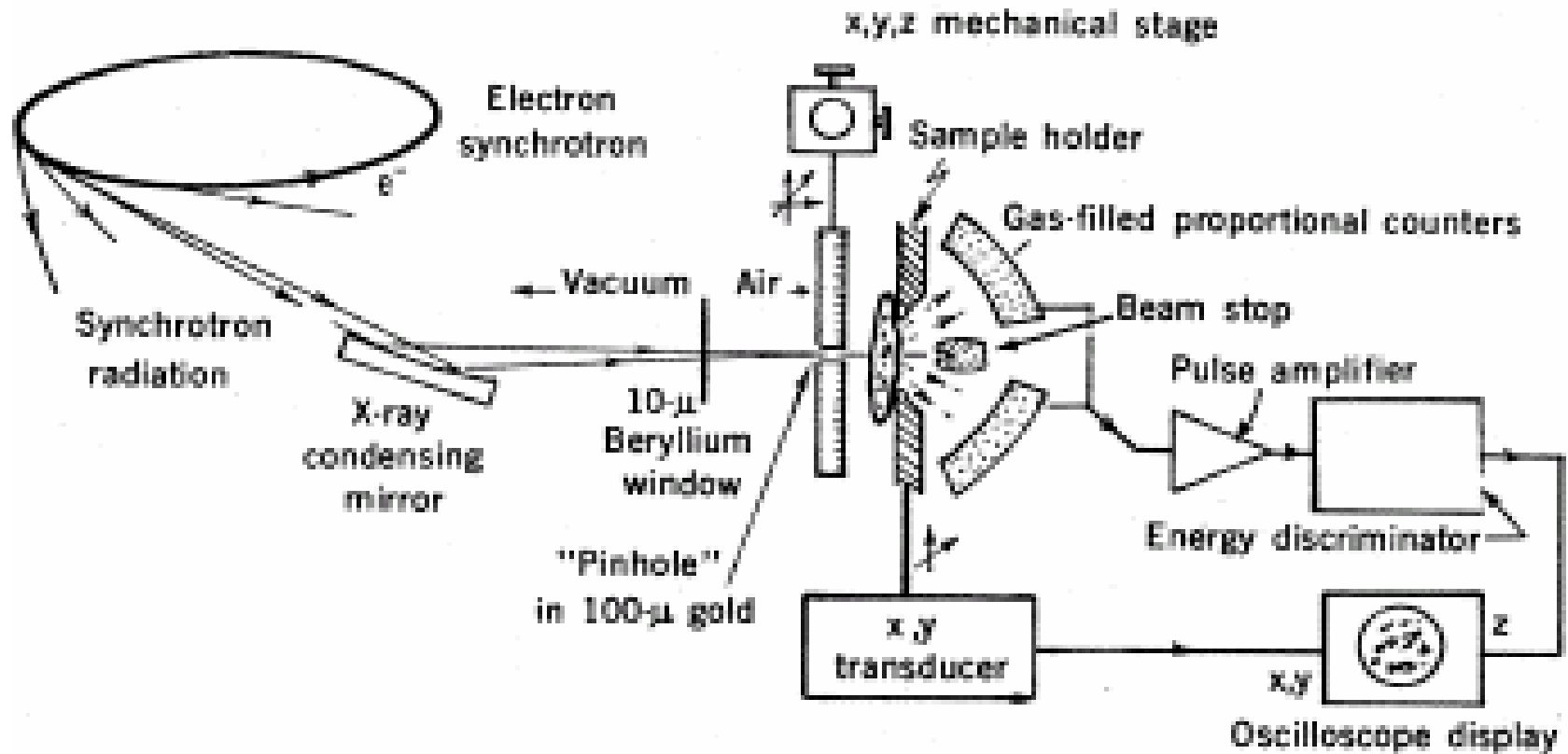
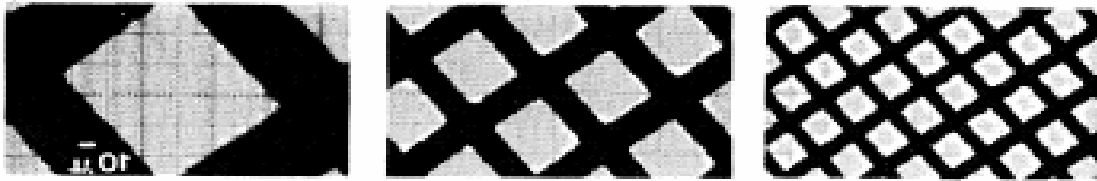


FIG. 1. Scanning x-ray microscope.

Horowitz and Howell A Scanning X-ray Microscope using Synchrotron Radiation Science, 178, 608 (1972)

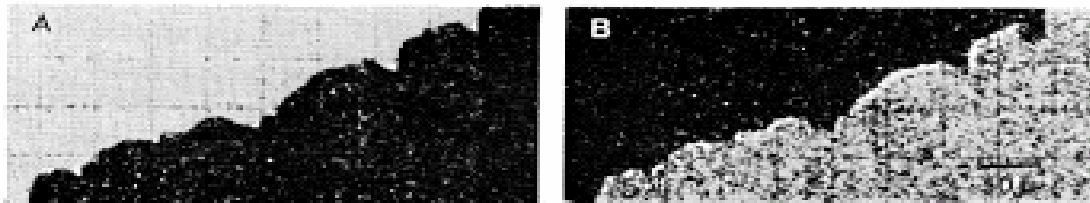


Horowitz and Howell 1-2 micron pinhole collimator



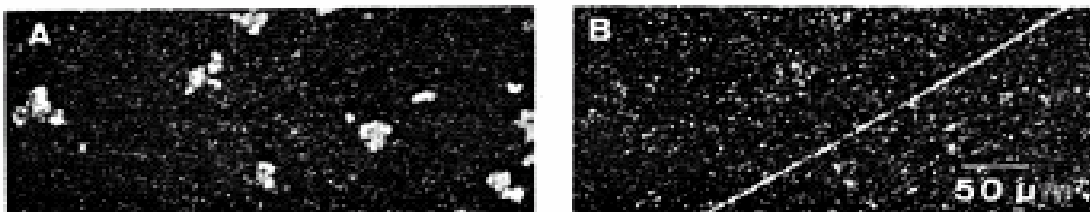
transmission

Fig. 2. Transmission micrographs of a 200 mesh per inch (80 grids per centimeter) copper grid at three different magnifications. The faint horizontal and vertical lines in these micrographs are from the oscilloscope graticule.



transmission and
Al fluorescence

Fig. 3. An aluminum foil 10 μ thick viewed: (A) in transmission and (B) in aluminum K fluorescence.



S and Si
fluorescence

Fig. 4. A sample consisting of sulfur dust and a 2- μ silicon whisker viewed: (A) in sulfur K fluorescence and (B) in silicon K fluorescence.

Scanning microscopy

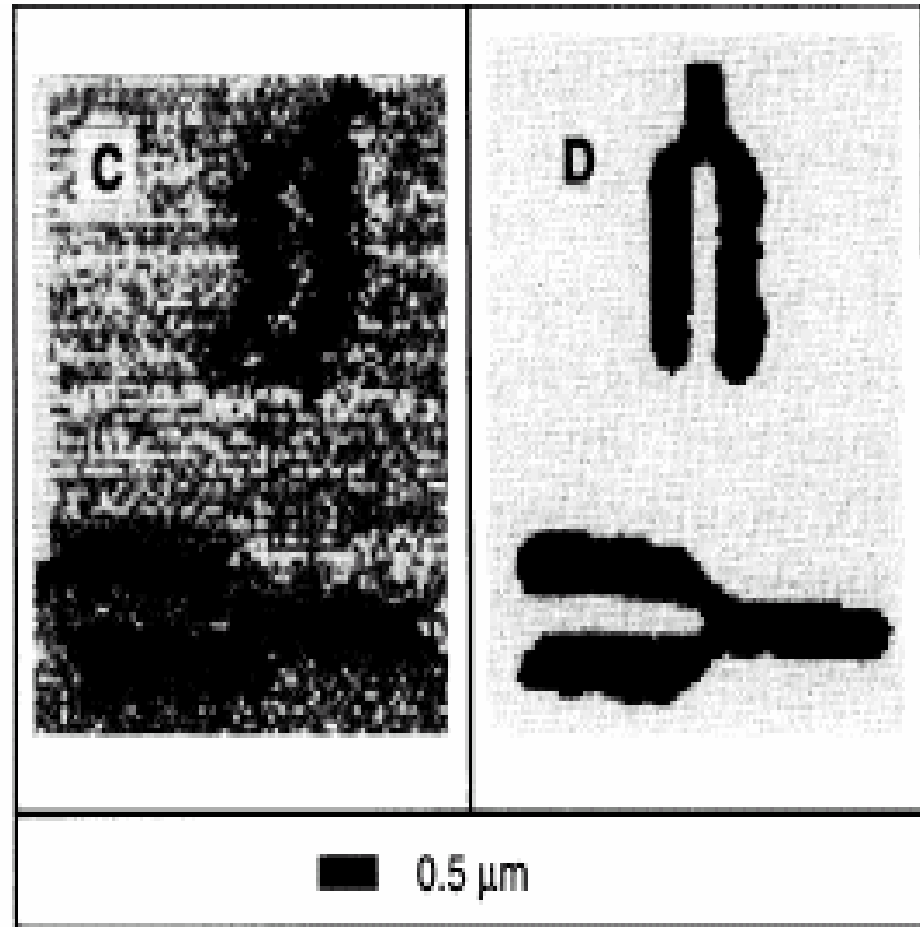
- Scan specimen (or probe) mechanically
 - Collect image pixel by pixel
- Detect
 - transmitted x-rays (STXM),
 - fluorescence (SXRF)
 - photoelectrons (SPEM)
 - visible light (SLXM)
 - diffracted X-rays
- Size of microprobe determines resolution
 - here $\sim 2 \mu$, formed by pinhole
- Brightness limited
- Scan parameters determine object area, “magnification”

Comments on the formation of the probe

- Major types:
 - Pinholes; Tapered capillaries; Waveguides
 - Mostly for high energy X-rays
 - Mirrors
 - Normal incidence (multilayer) - <200 eV
 - Grazing incidence 3 – 30 KeV
 - Lenses
 - Compound refractive – high energy
 - Zone plates 200 eV – 20 KeV

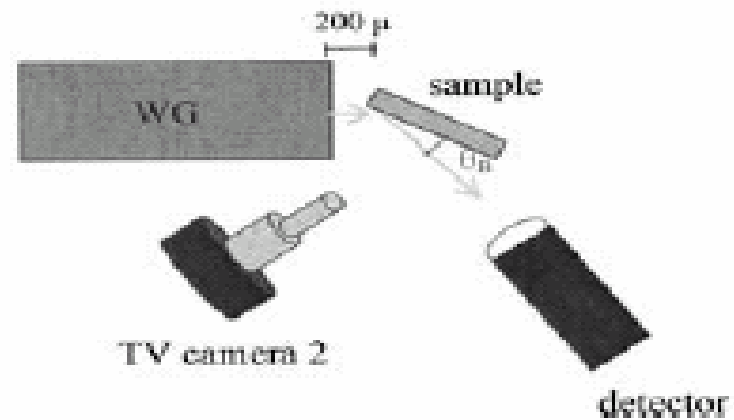
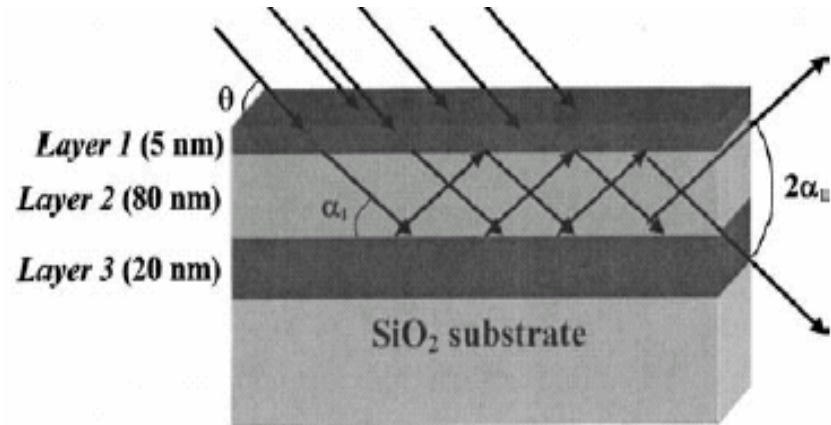
Tapered capillaries

D. H. Bilderback, S. A.
Hoffman, & D. J. Thiel,
Science 263, 201 (1994)



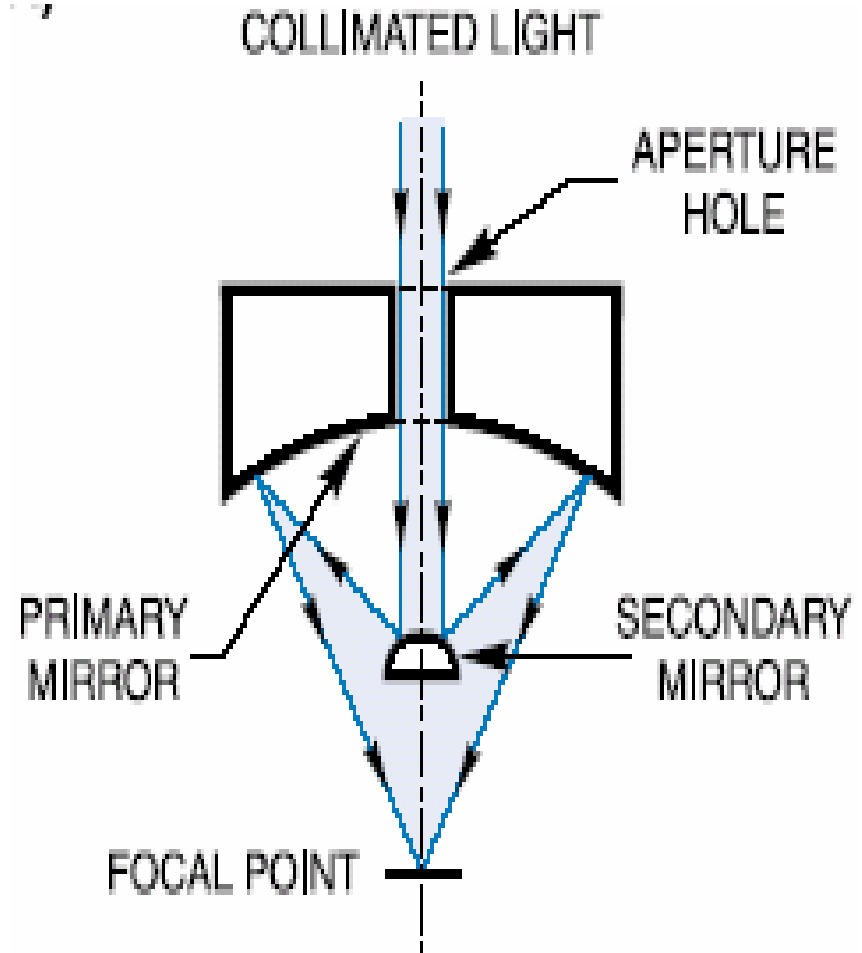
Waveguides

A. Cedola, S. Lagomarsino,
F. Scarinci, M. Servidori,
V. Stanic, J. Appl. Phys.
98, 1662 (2004)



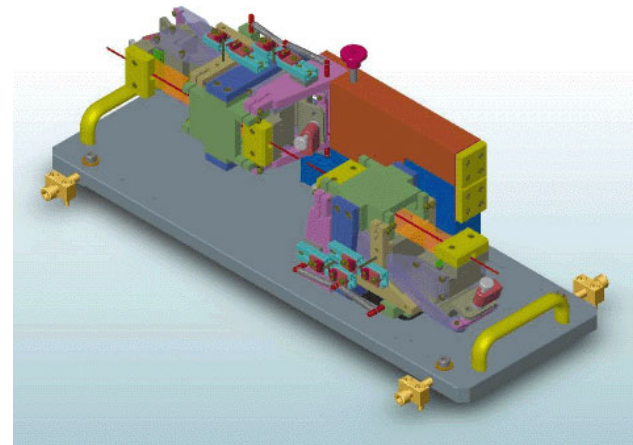
Mirrors - normal incidence

- Schwarzschild objective
- Multilayer coating:
 - Spiller
- First attempt: R.-P. Haelbich, W. Staehr, C. Kunz, HASYLAB 1980
- Hoover - NASA
- MAXIMUM
- SuperMAXIMUM



Mirrors - grazing incidence

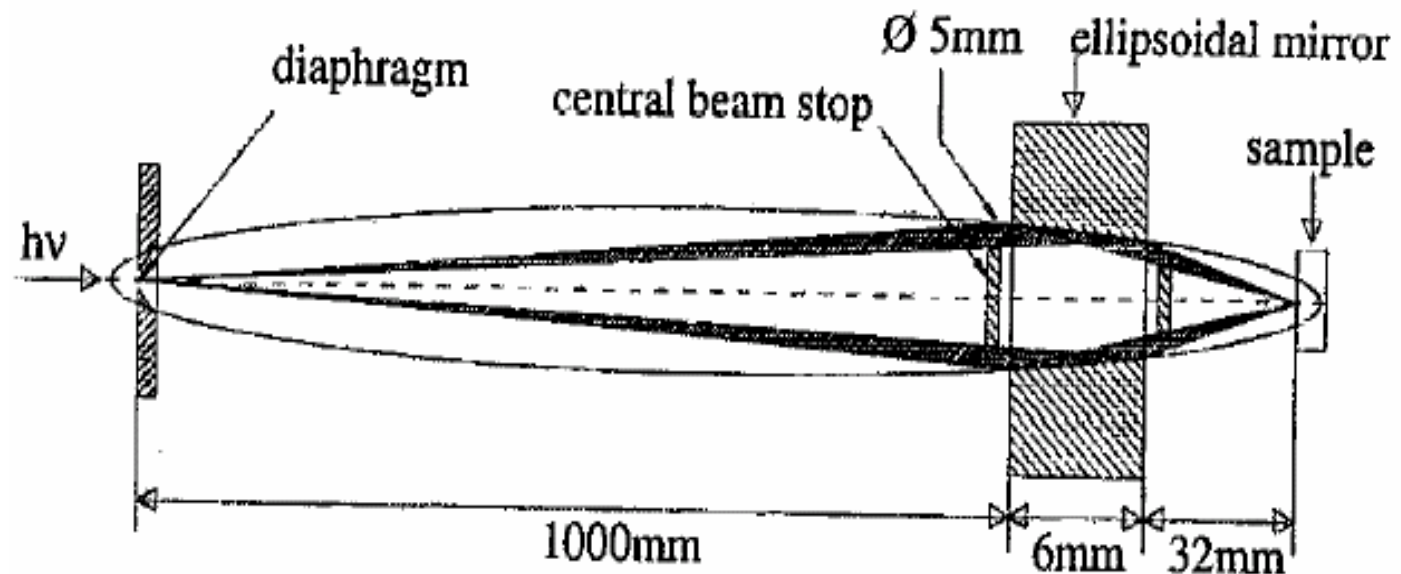
- achromatic!
- Kirkpatrick-Baez:
separate x and y
focusing
- Elliptical bending
- 100 nm focal spot (A.
Freund et al. ESRF)



Mirrors - grazing incidence

- Ellipsoids:

J. Voss, H. Dadras, C. Kunz, A. Moewes, G. Roy, H. Sievers, I. Storjohann, and H. Wongel, *J. X-ray Sci. Technol.* 3, 85 (1992).



Parabolic refractive lenses ESRF/Aachen collaboration

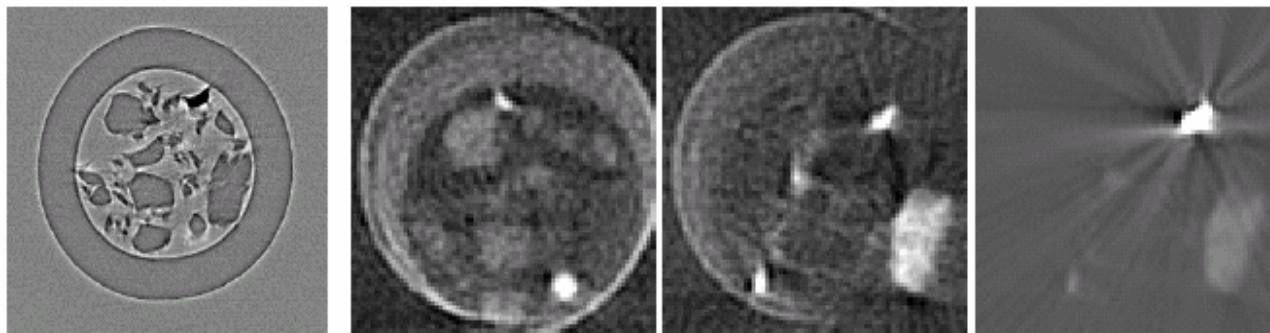
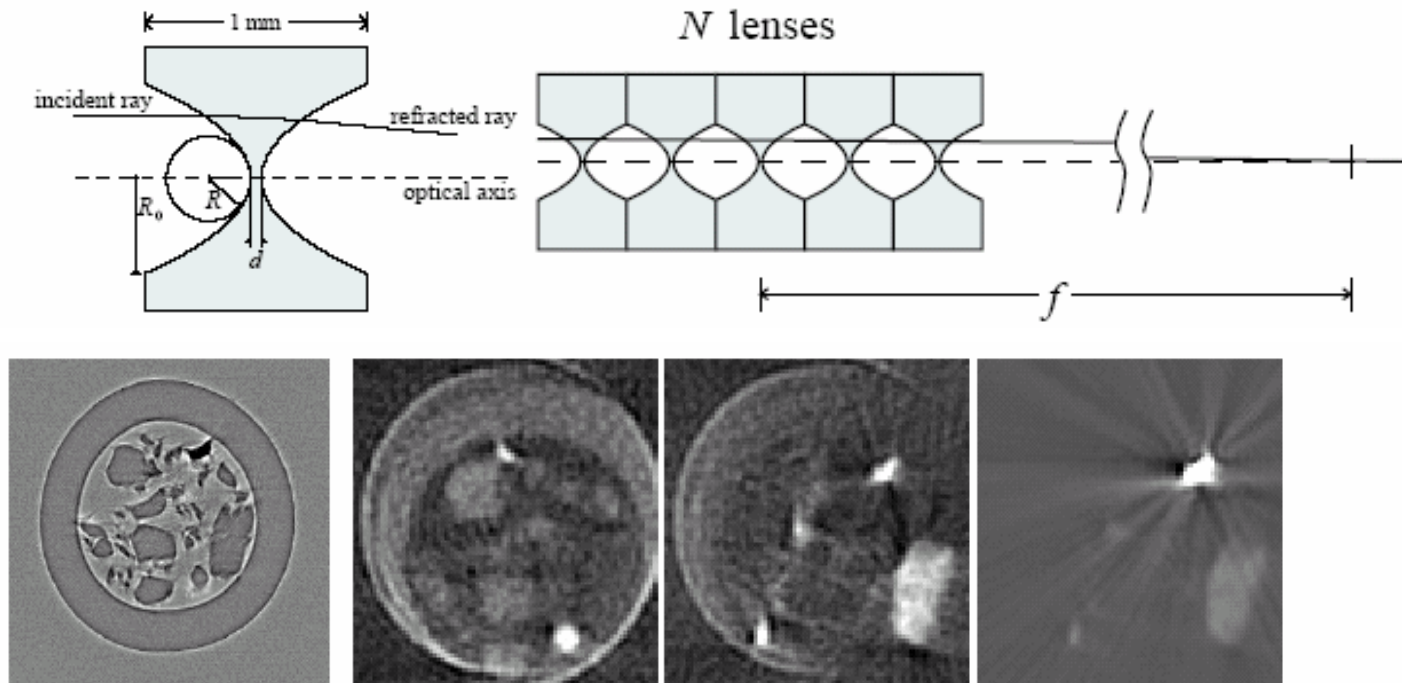
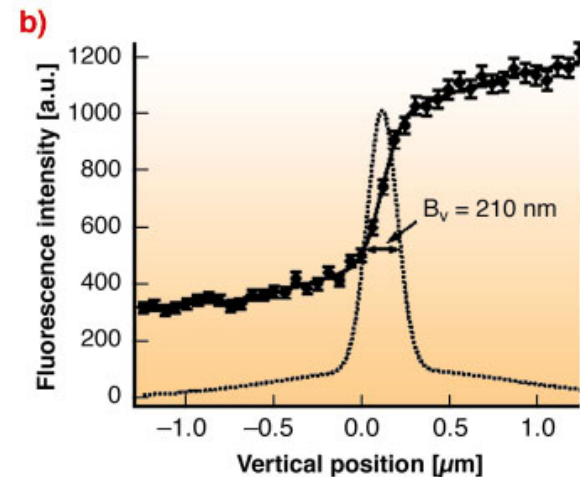
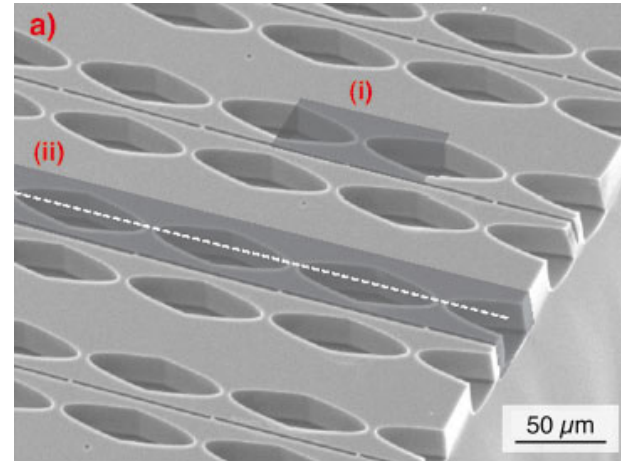


Figure 2: Results a combined transmission and fluorescence microtomography study. The sample consisted of different particles in a glass capillary (inner diameter 100 μm . The capillary wall as well as the particle outlines are clearly visible in the transmission tomogram of a slice in the sample (*far left*). The three images on the right are fluorescence tomograms of the same slice for different energies of the fluorescence radiation, namely Zr-K α (*left center*), K-K α (*right center*), and Fe-K α (*far right*).

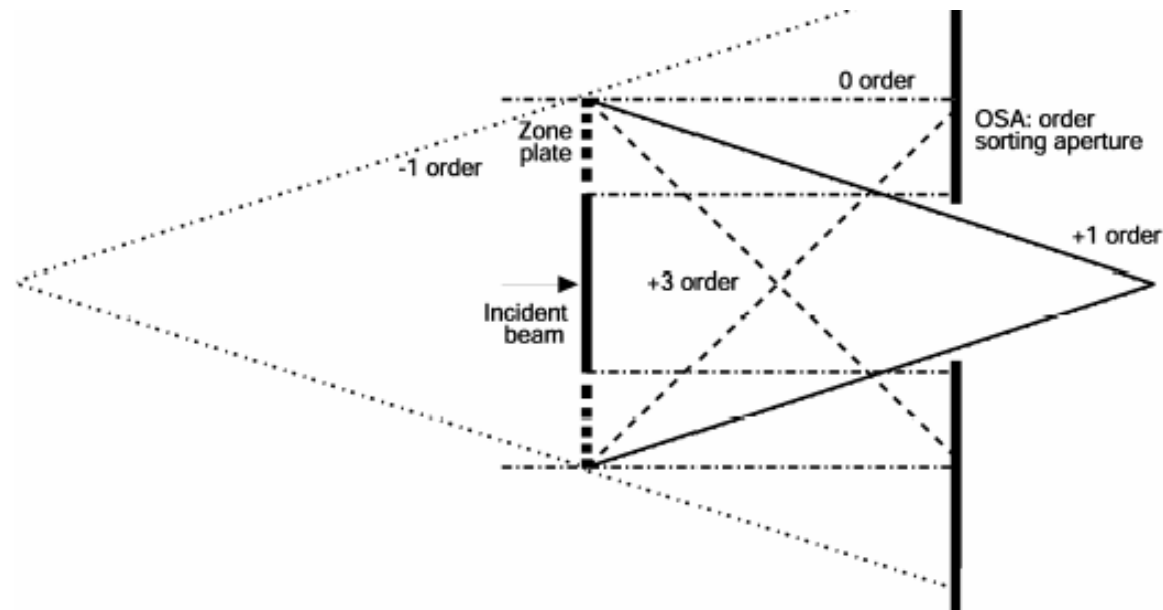
Parabolic refractive lenses

- Other efforts:
cylindrical lenses by
microfabrication
- Heat load not problem!
- Alignment much easier
than K-B
- Chromatic
- Figure: C. G. Schroer et
al., APL 82, 1485 (2003)



Zone plates

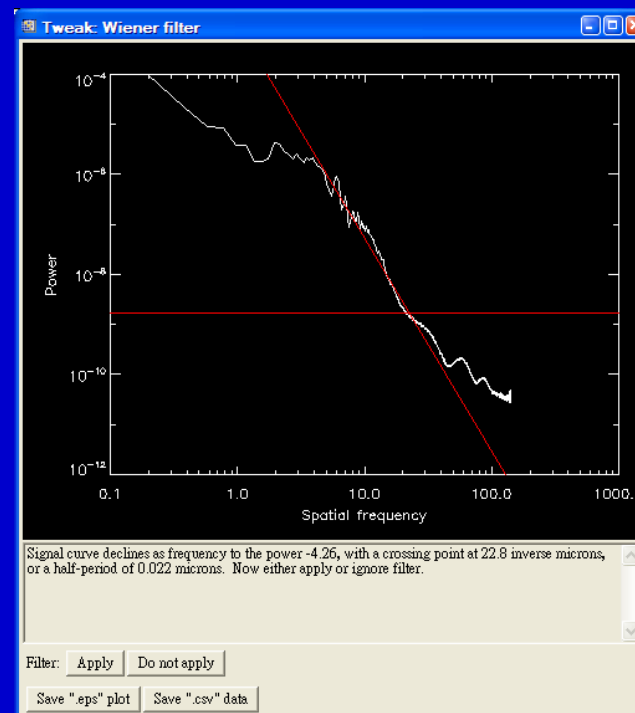
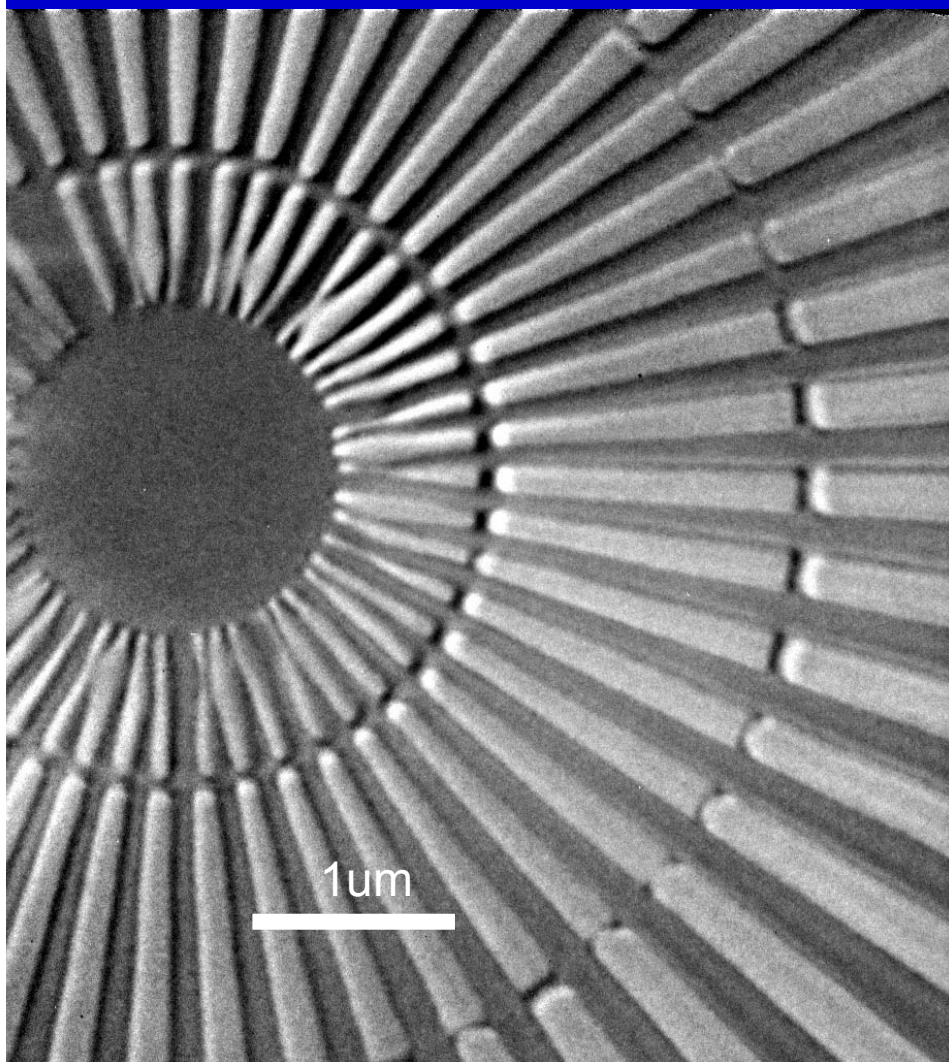
- Central stop and Order Sorting Aperture for forming microprobe and removing other orders
- No spherical aberrations!
- But chromatic!



Efforts at XRADIA

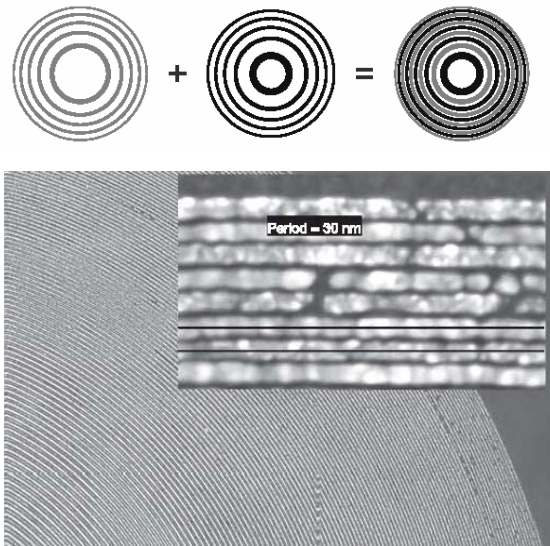
- $\delta r_n \sim 100$ nm, 1650 nm thick Au (for up to 24 KeV)
- $\delta r_n \sim 50$ nm, <700 nm thick Au (for up to 9 KeV)
- $\delta r_n \sim 40$ nm, <150 nm thick Au (for up to 1.4KeV)
- Working on achromatic X-ray lens
 - (zone plate plus non-focusing corrector)

Gold Spoke Pattern Imaged by 3rd Diffraction Order of Zone Plate

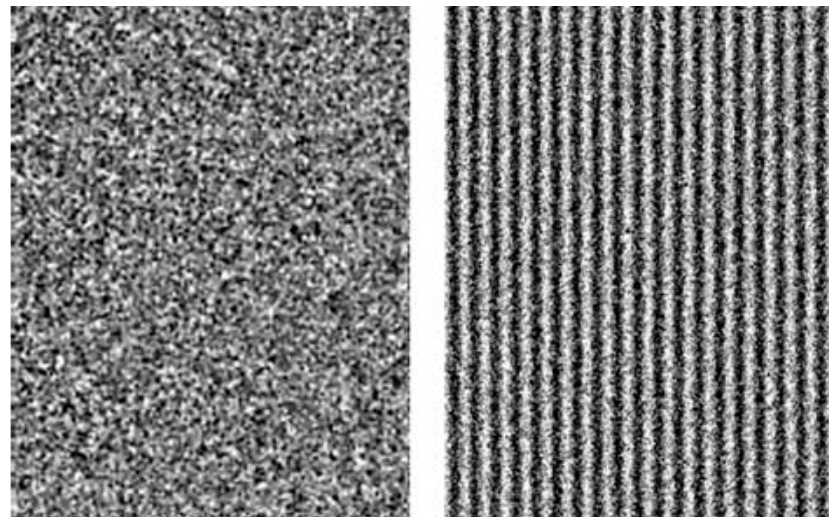


$E = 8 \text{ keV}$
Exposure time : 10 mins
Resolution: About 25nm
FOV : 5μm x 5μm

Zone Plate Lenses with Better than 15-Nanometer Spatial Resolution

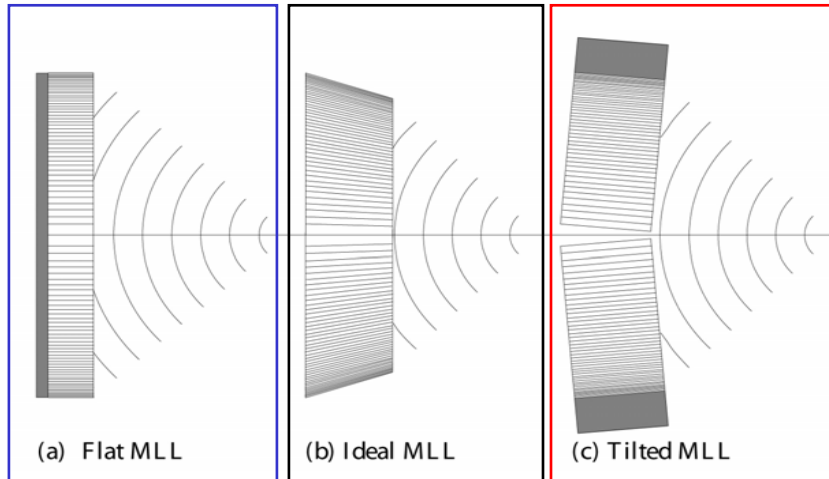


Overlay technique with separate e-beam lithography patterns for odd and even zones achieves 30-nm zone period (center-to-center) with high quality (e.g., placement accuracy of 1.7 nm).



Soft x-ray images taken with the CXRO XM-1 full-field imaging microscope at the ALS (Beamline 6.1.2). Comparison of images of a 15.1-nm test object with the previous 25-nm (left) and the new 15-nm (right) zone plates illustrates the improved spatial resolution achievable.

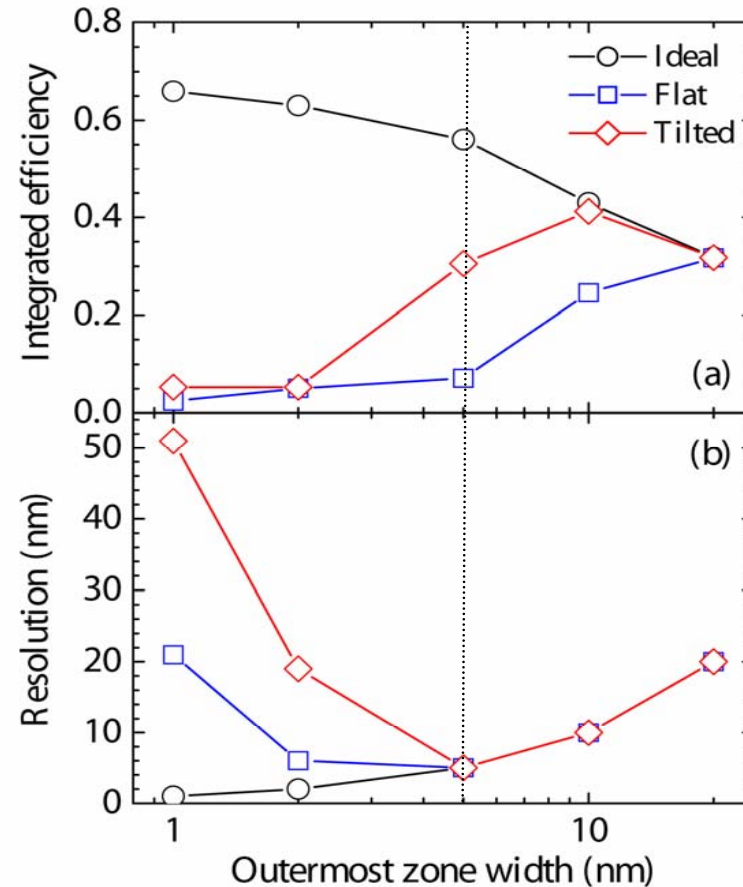
Where is the resolution limit for x-ray focusing (Diffractive Optics)?



- Ideal structure:
 - Resolution approaching 1 nm feasible,
 - Diffraction efficiency (2D) > 50%
- Tilted MLL: $\delta = 5$ nm feasible

- Locally 1D N-wave CWT valid to ~ 1 nm
- Beyond:
 - What is the effect of Borrmann-Fan on Phase?
 - When is curvature of zones required?

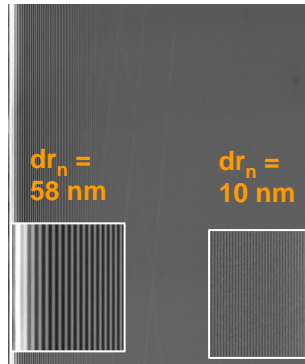
Calculations for 1D MLL



Kang et. al, PRL, 96, 127401 (2006)

Multilayer Laue Lens – Concept

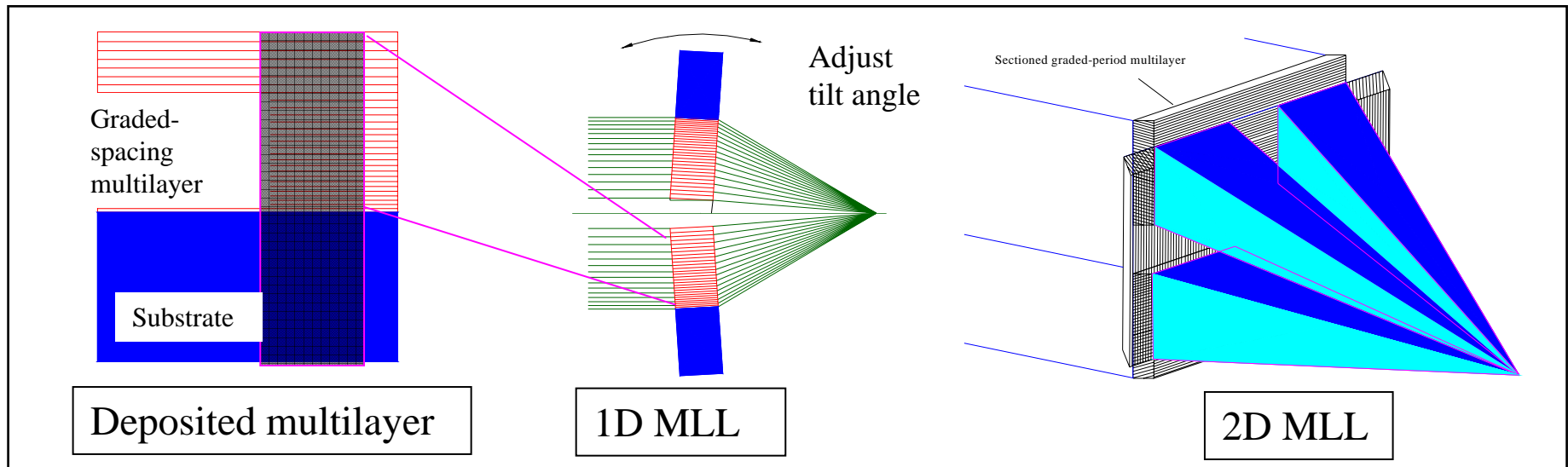
- Deposit varied depth-graded multilayer on plane substrate (**thinnest structures first**)
- Section to 5-20 μm depth
- Assemble into a linear MLL
- Assemble two linear MLL's into a 2D MLL.



Material: WSi_2/Si

Total deposition thickness: 12.4 μm

d-spacing: 10 – 58 nm



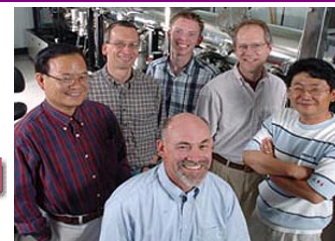
Cross-divisional team (MSD/CNM/XFD)
capitalizes on strengths of ANL science
and facilities

2005 R&D 100 Award

The 43rd Anniversary



Awards



X-ray focusing with MLL sections, $dr_N = 15$, $dr_N = 10$ nm

Sample A: $dr_N = 15$ nm

Sample B, C: $dr_N = 10$ nm

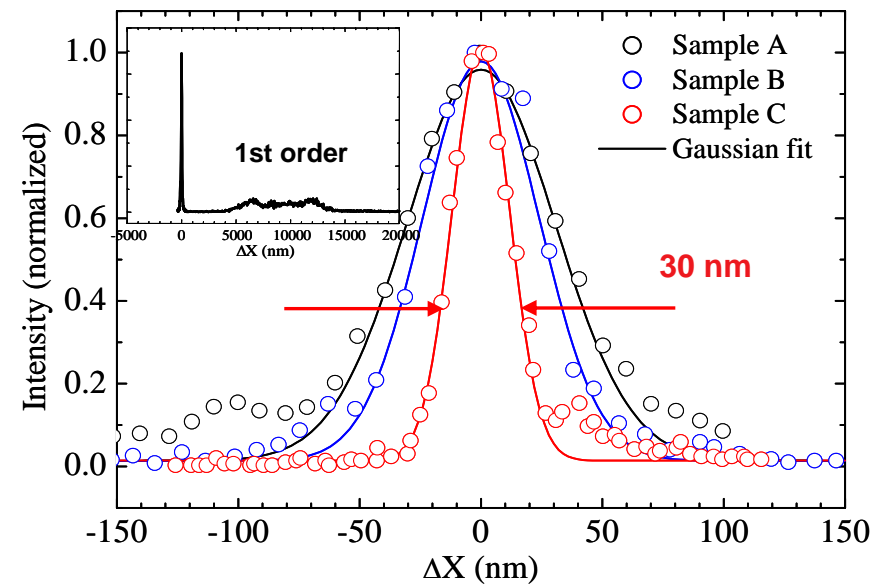
NA-limited resolution:

Sample A: 57 nm (27% NA)

Sample B: 44 nm (23% NA)

Sample C: 24 nm (41% NA)

Resolution measurement

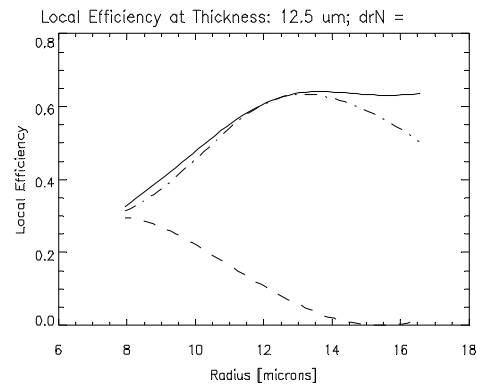
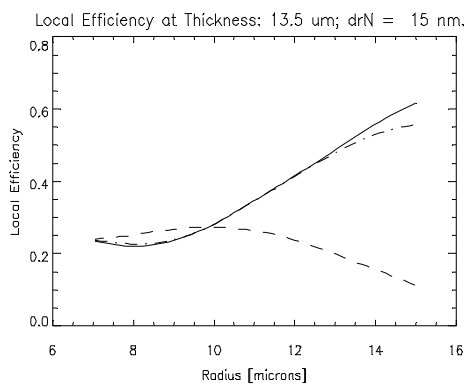


Photon Energy: 19.5 keV

Measured Resolution: **30 nm**

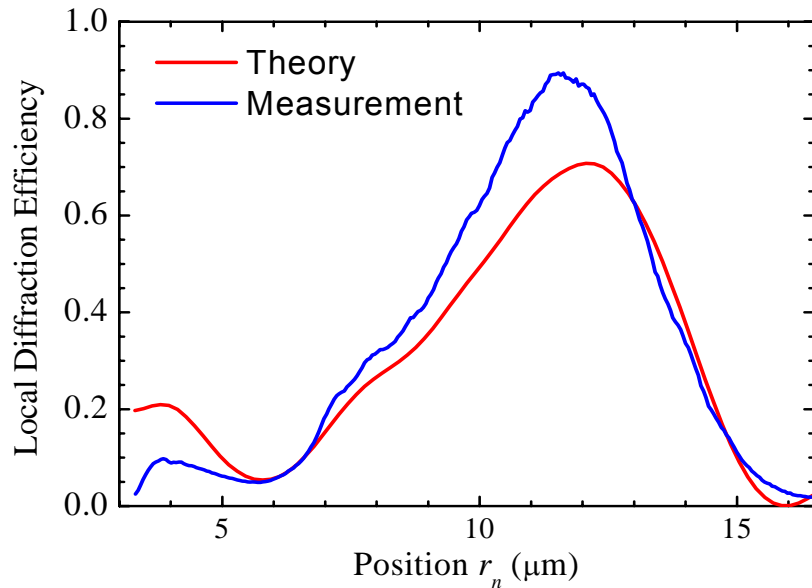
Diffraction Efficiency: **44%**

Kang et. al, PRL, Apr., 2006



X-ray focusing with MLL sections, $dr_N = 5 \text{ nm}$

Experiment and Theory (Coupled Wave Theory)



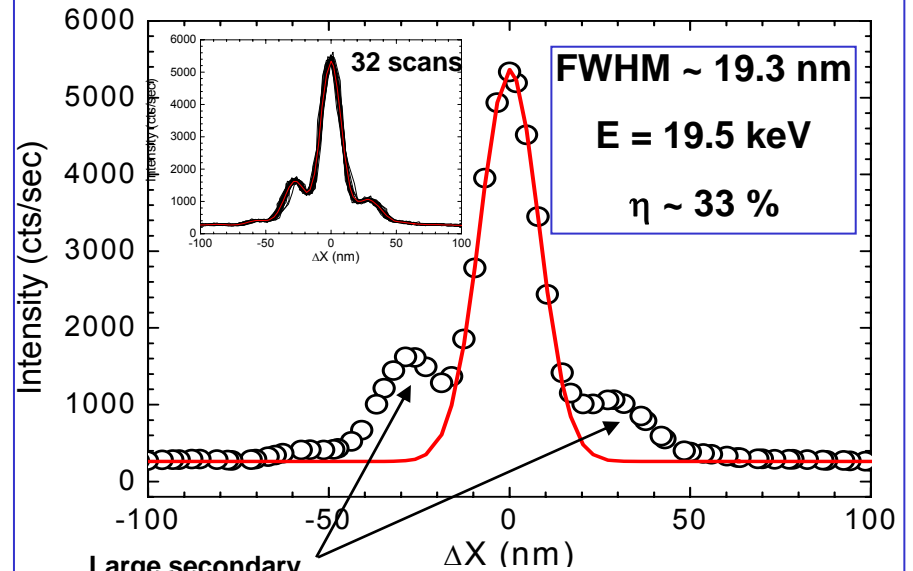
Radial change of local efficiency

Calculated integrated efficiency ~ 30 %

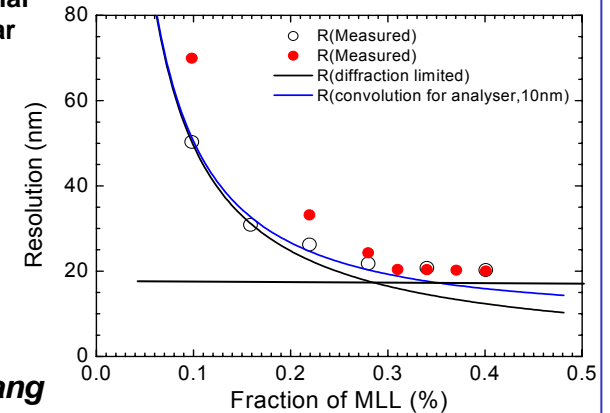
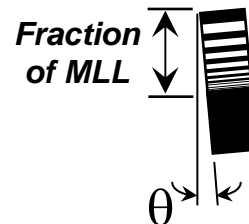
Measured Integrated efficiency ~ 33 %

(unpublished)

Resolution measurement



Large secondary maxima due to partial structure and linear geometry

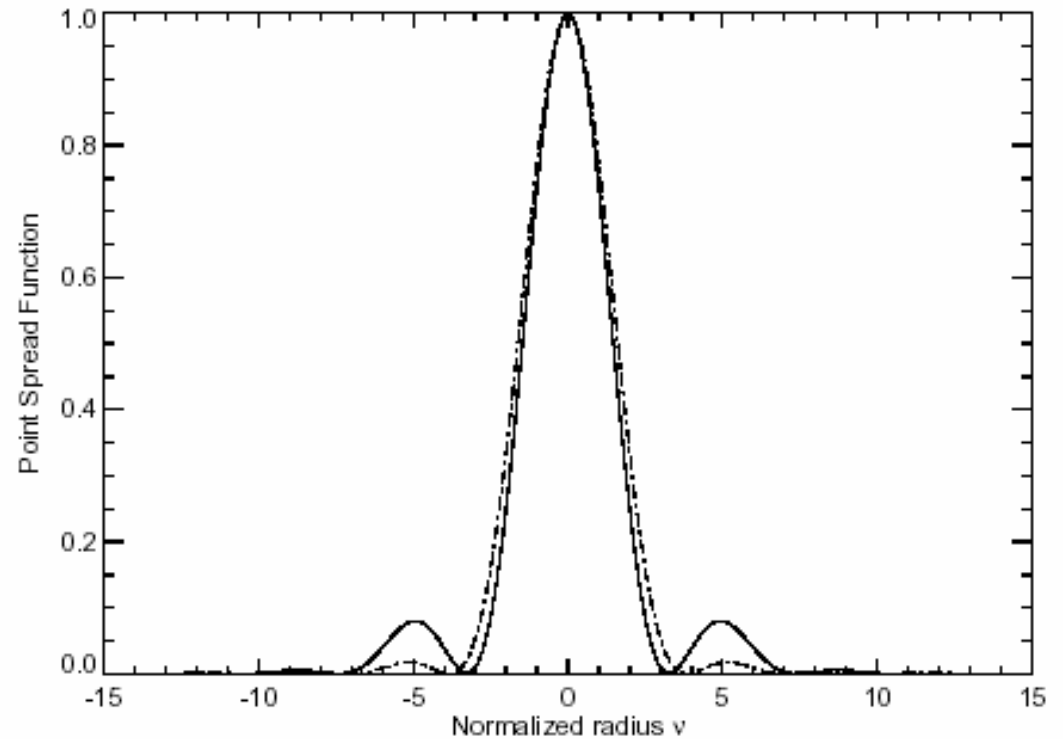


Courtesy H.C. Kang

- Mirrors and lenses demagnify small source
 - For microprobe, off-axis aberrations irrelevant!
- Diffraction-limit: focus size $\propto \lambda/NA$
- Strehl-ratio: What fraction of photons within focus?
- Depth of focus and working distance

Shape of focus

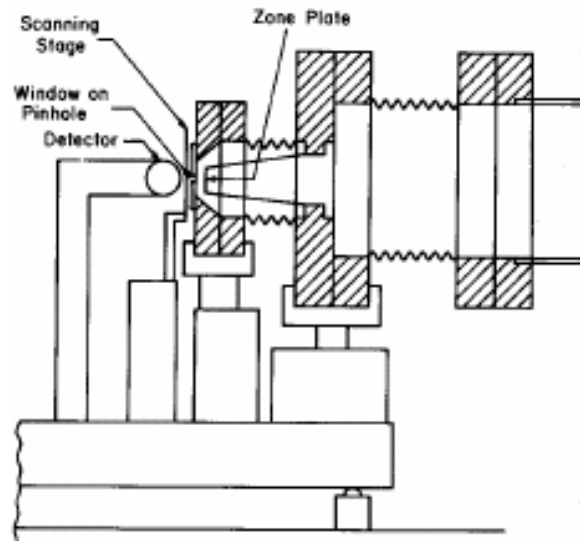
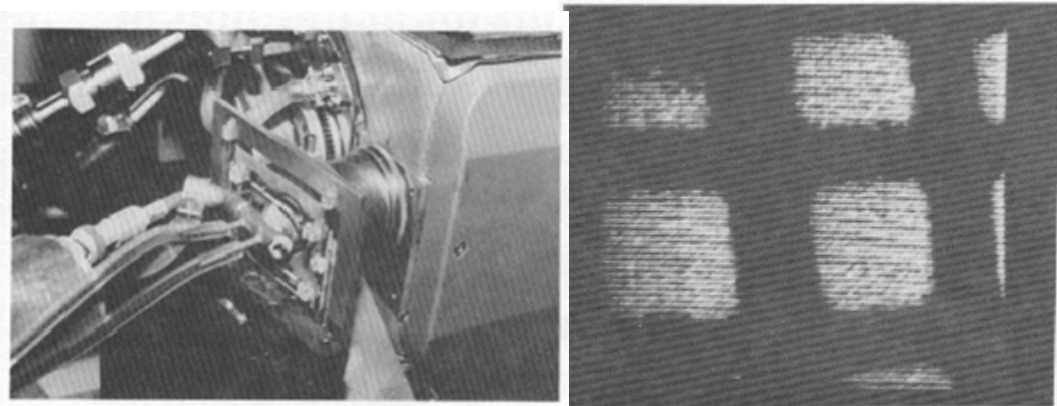
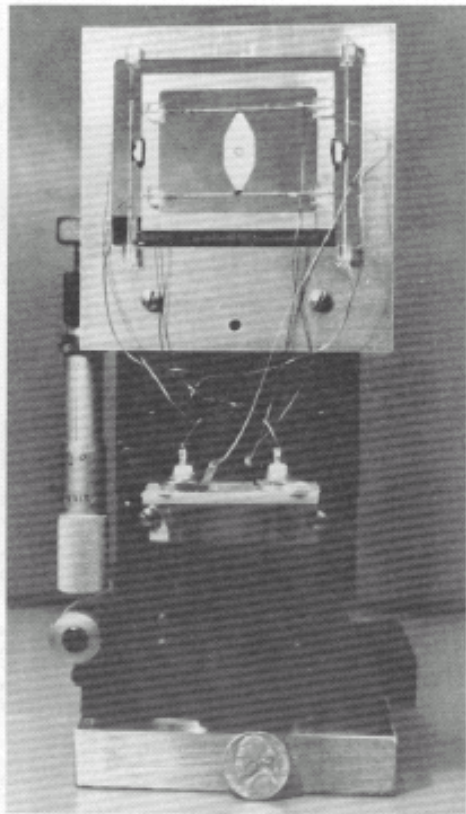
- Full coverage of aperture:
Airy pattern
- Partial coverage (central
stop, ring, segment):
increased secondary rings
- Apodization



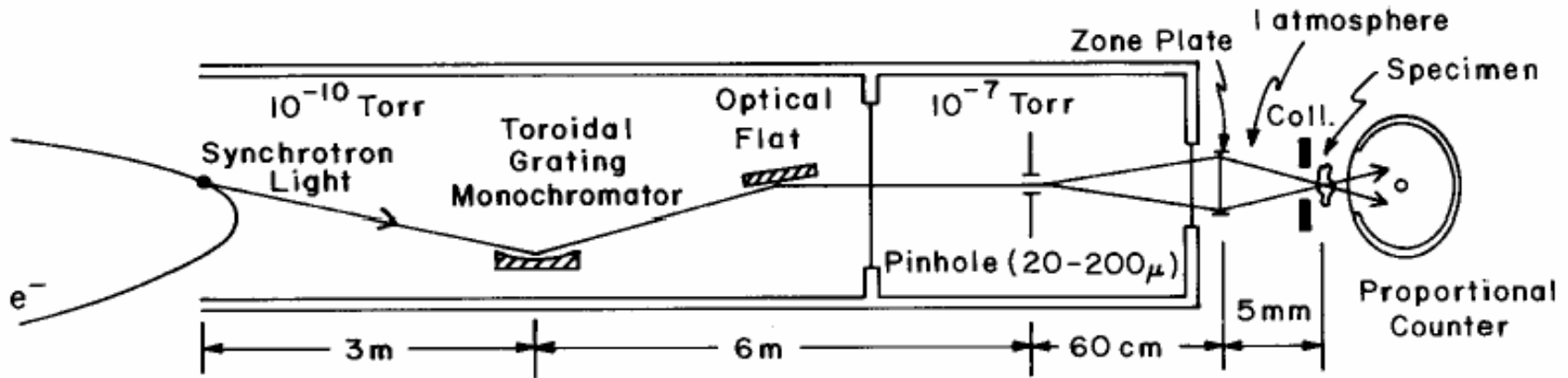
1979

Plans for a scanning transmission X-ray microscope

J. Kirz, R. Burg and H. Rarback
Ann. NY Acad. Sci. 342, 135 (1980)

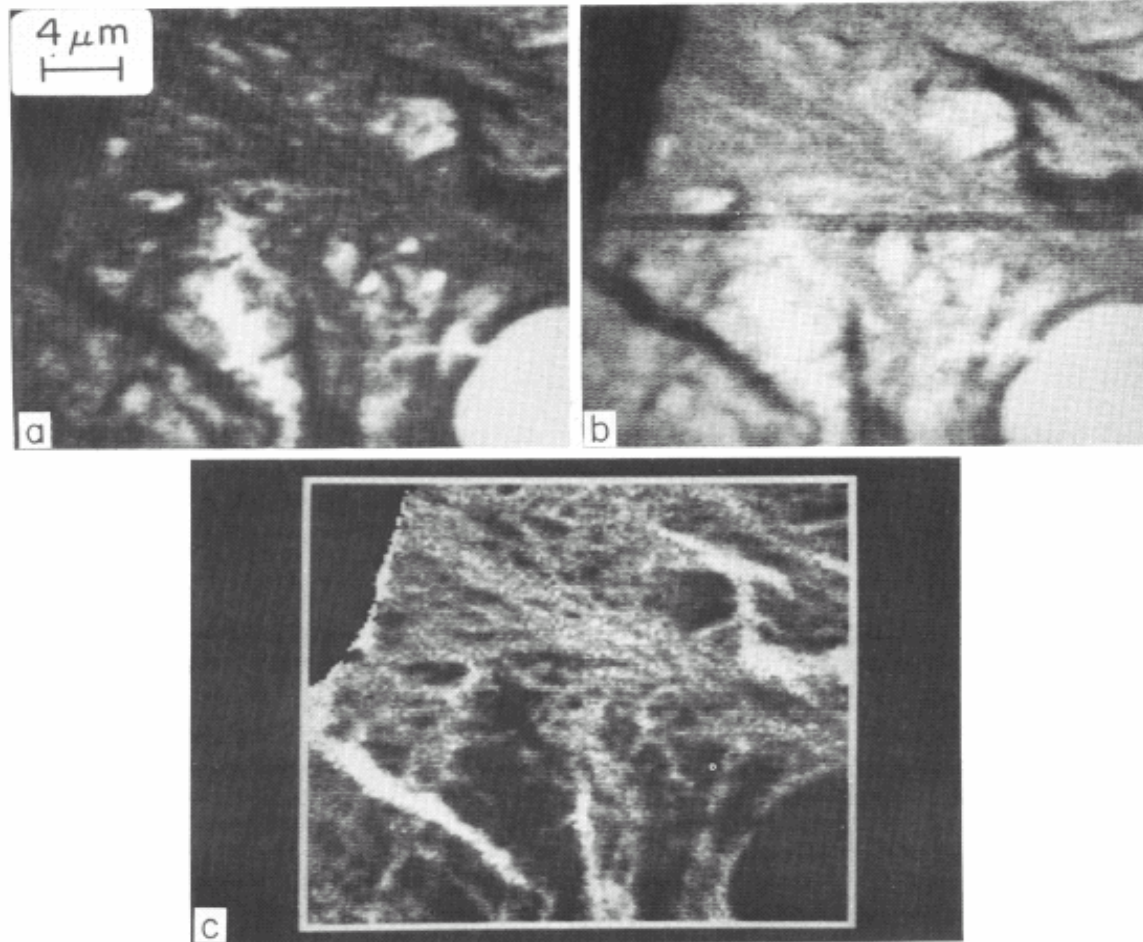
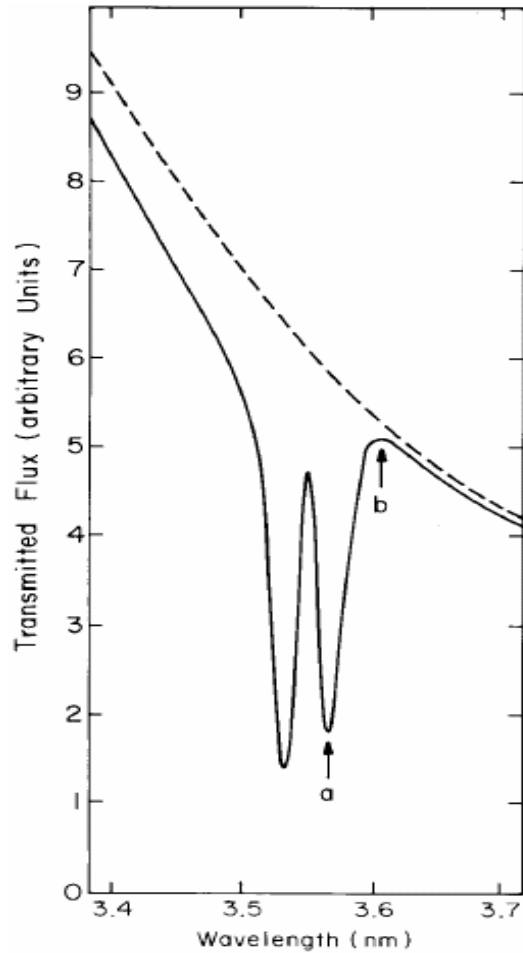


Scanning microscopy (STXM) 1983

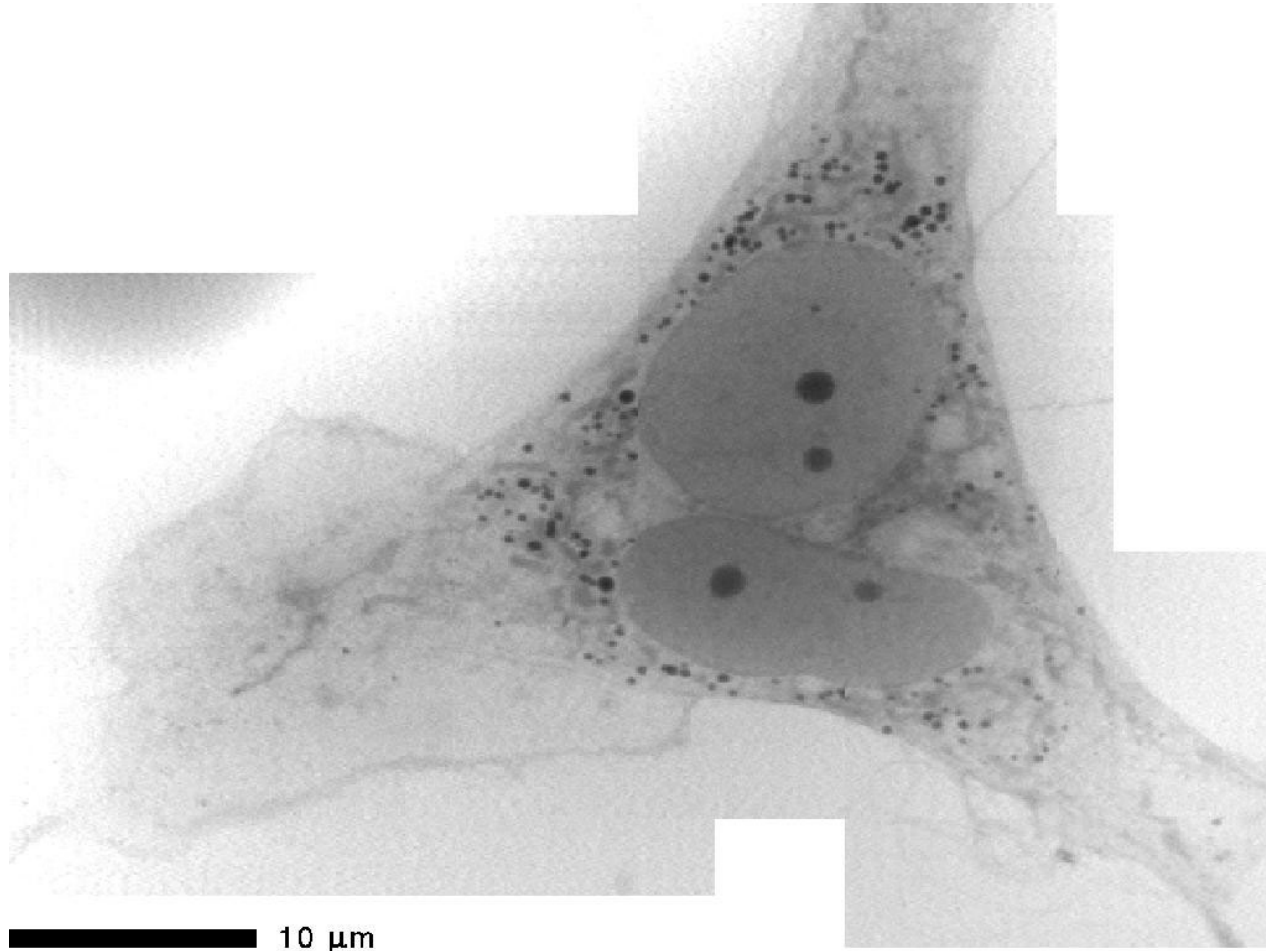


- Silicon nitride window
- Zone plate
- Proportion counter
- Scanning stage

Absorption microanalysis with a scanning X-ray microscope: mapping the distribution of calcium in bone
J. Kenney et al, J. Microsc. 138, 321 (1985)

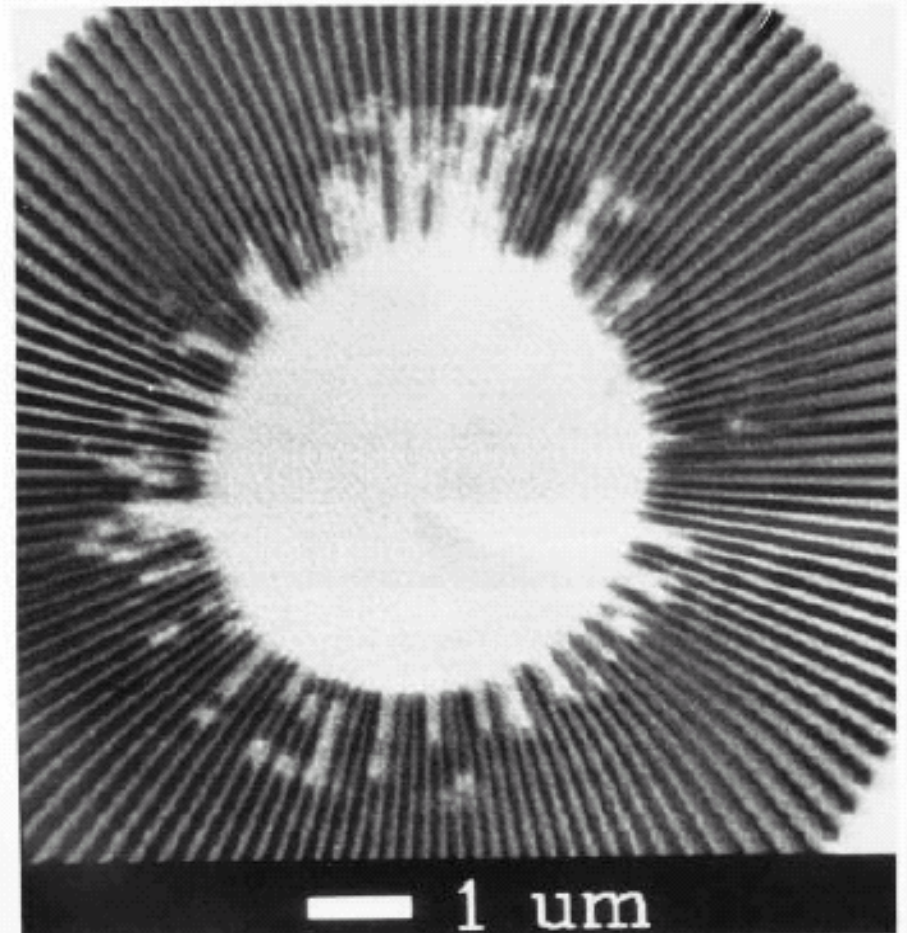
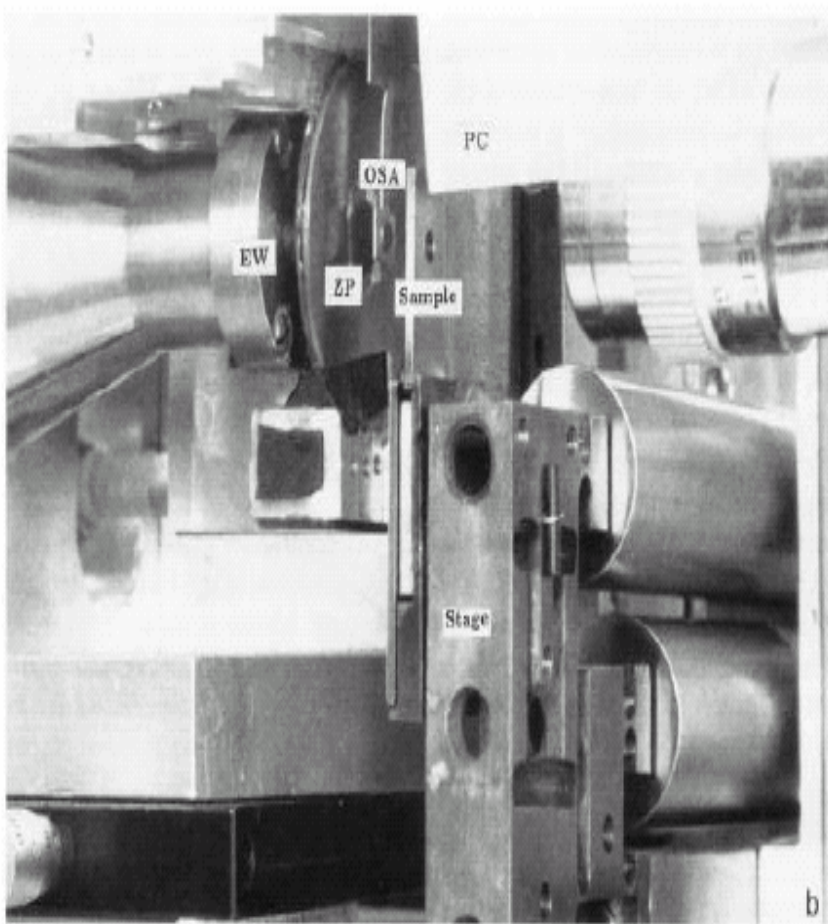


STXM – wet specimens 1986

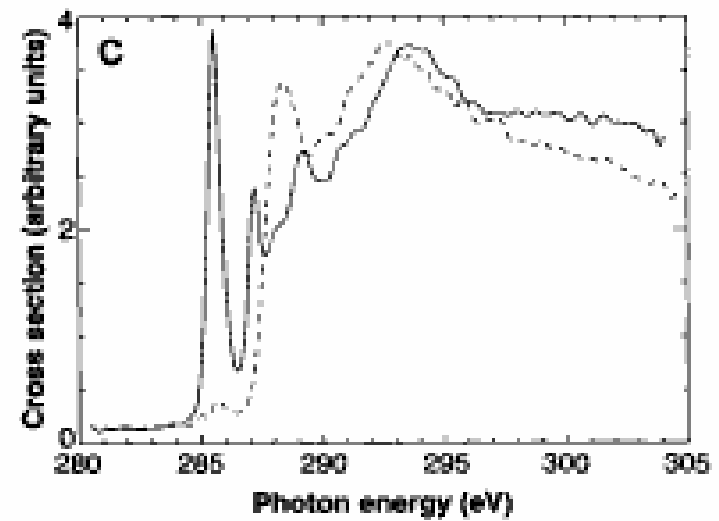
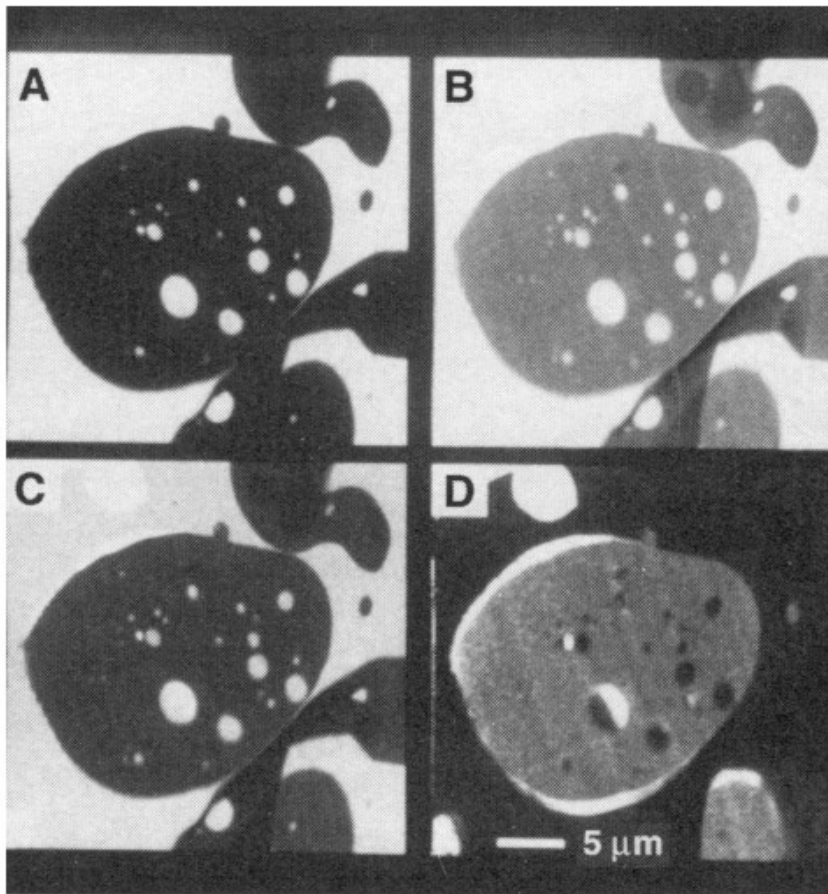


Gilbert thesis, '92

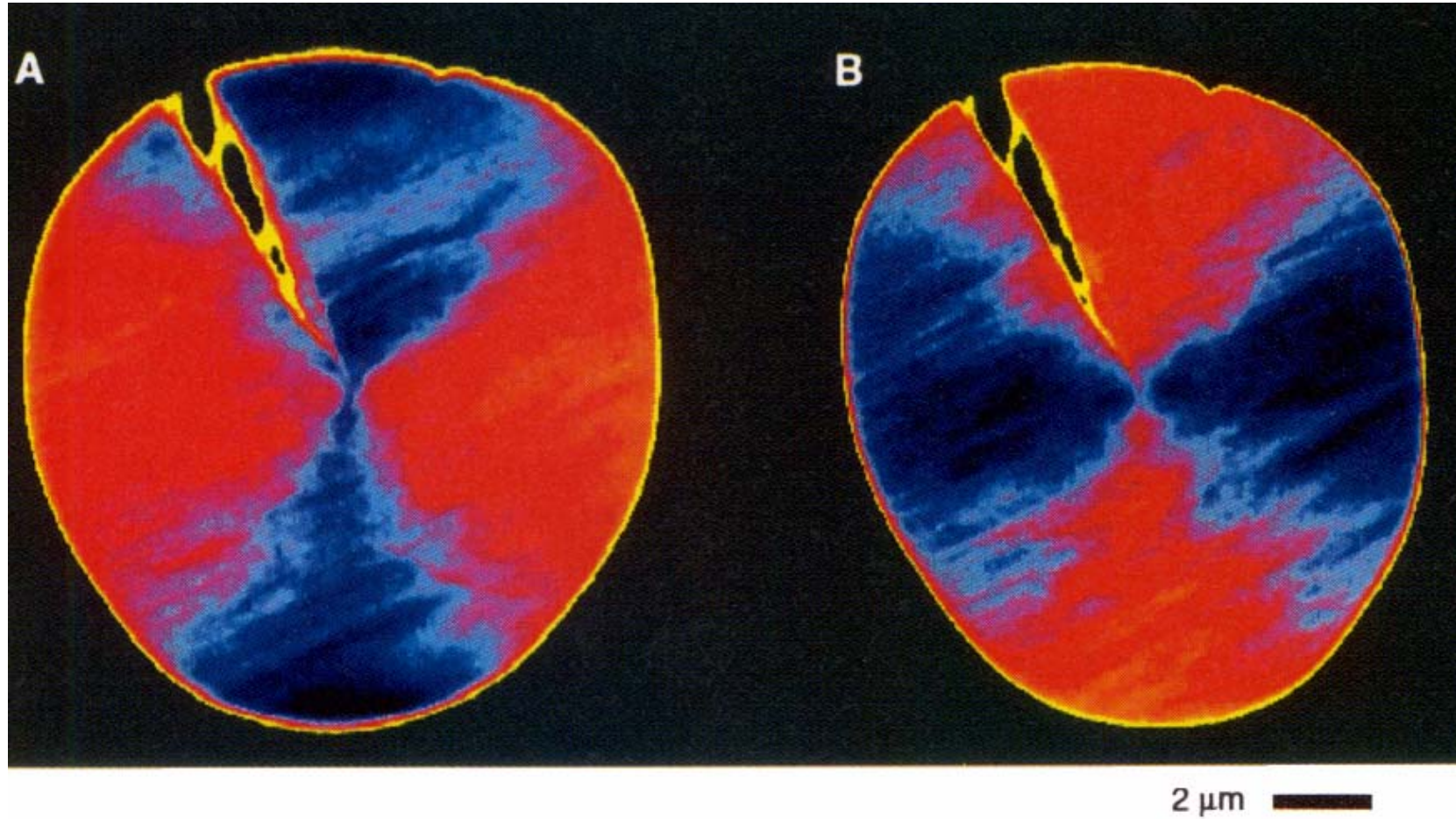
C. Jacobsen et al., Opt. Comm. 86, 351 (1991)
45 nm zone plate made at IBM/CXRO
X1 undulator, 340 eV



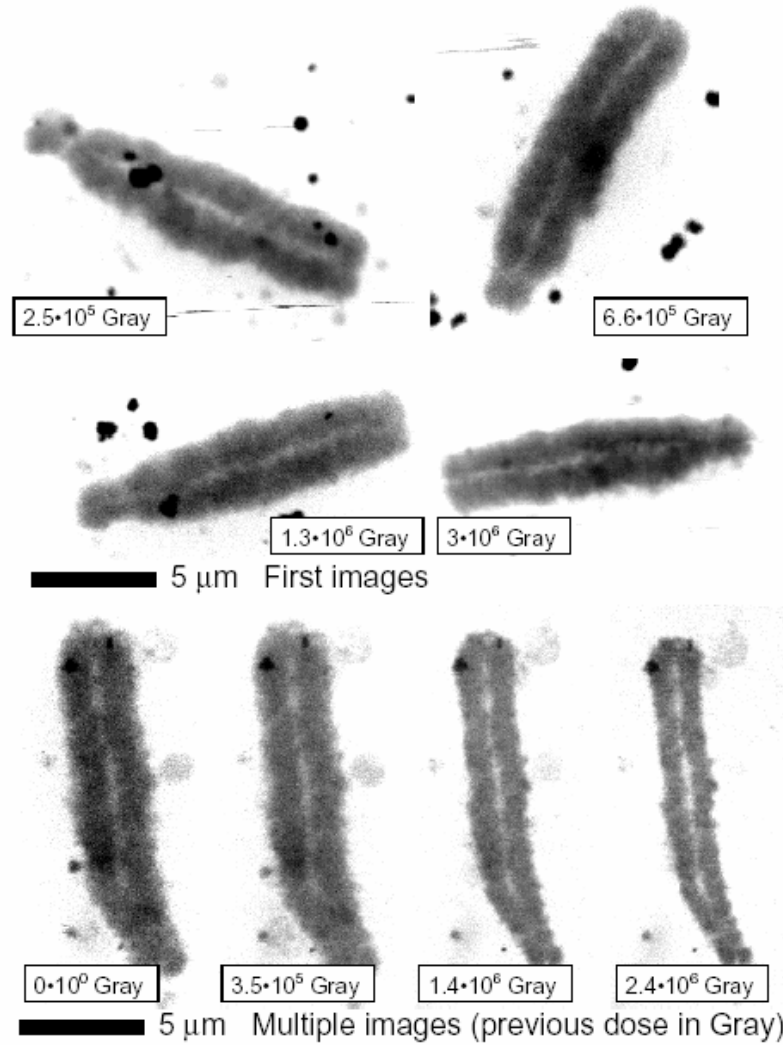
STXM 1992 spectromicroscopy



Linear dichroism microscopy Ade & Hsiao, NSLS 1993



Radiation damage studies, 1993

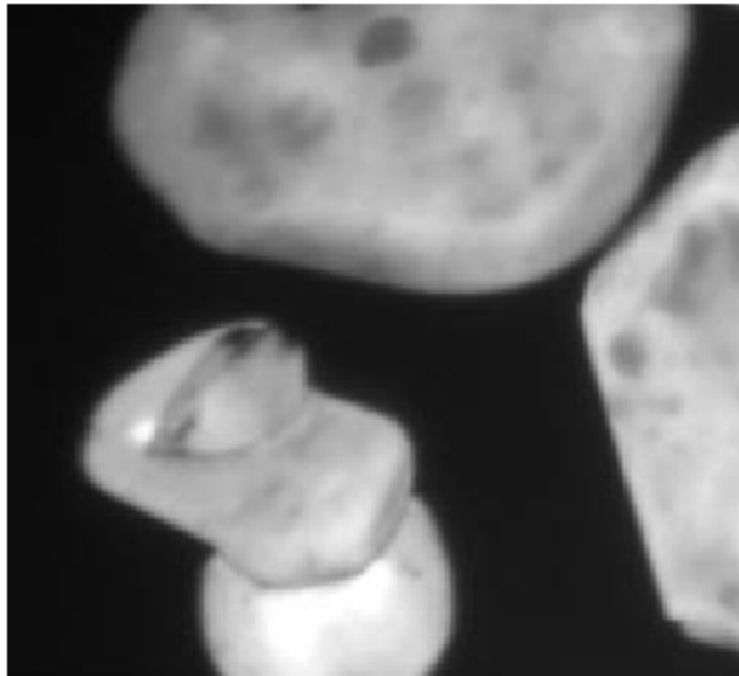


Williams et al. J. Microsc

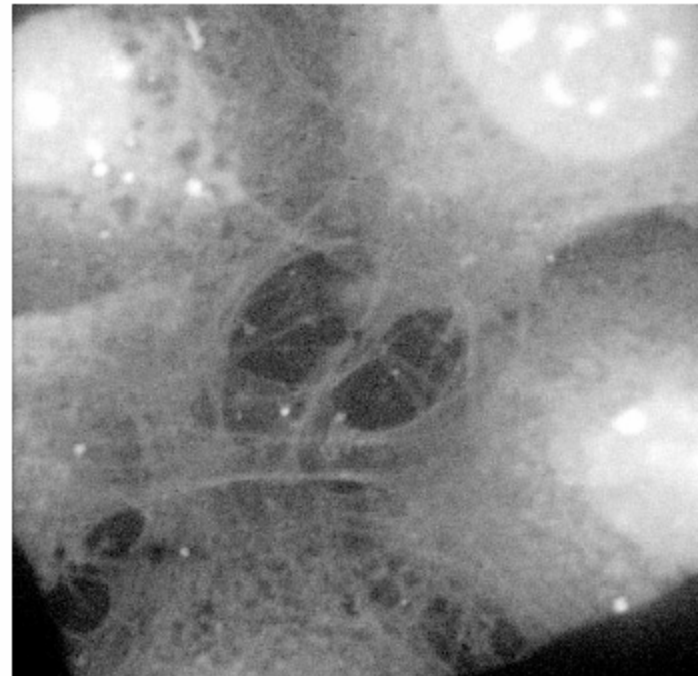
Visible light detection:SLXM

phosphor grains 1993

actin filaments 1994



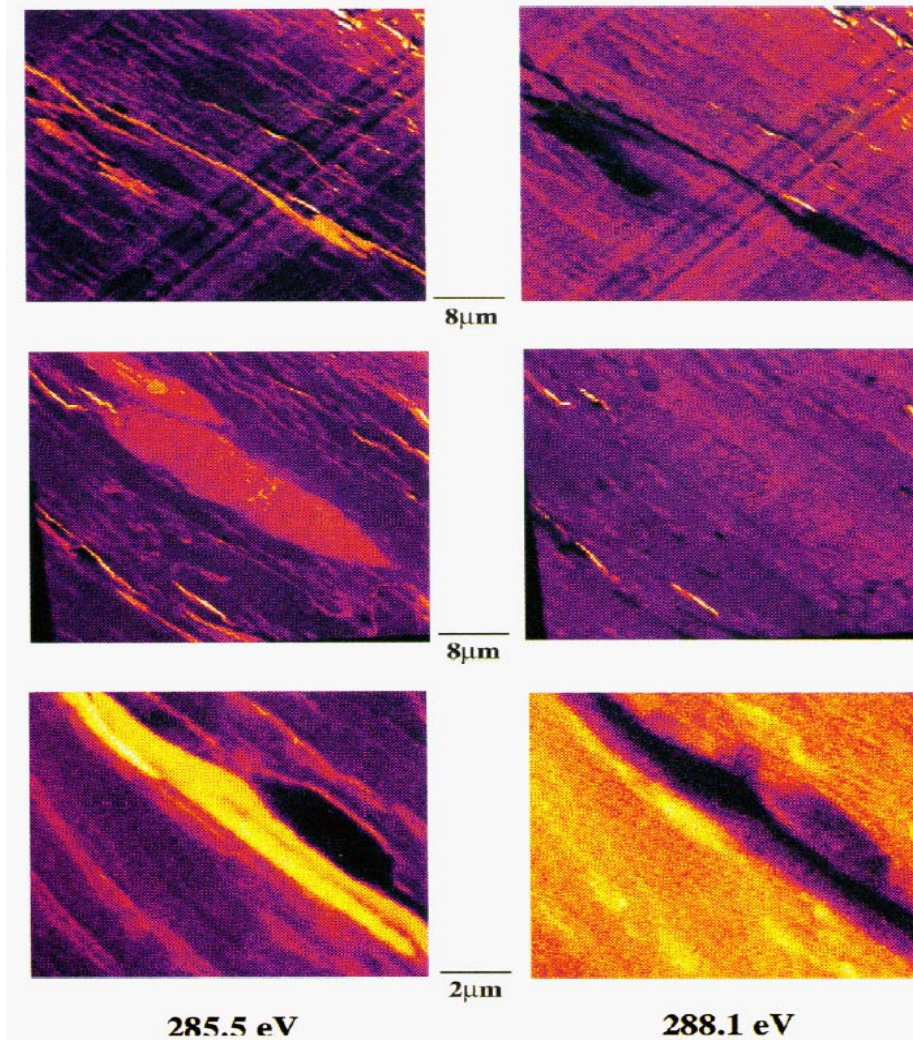
2 μm



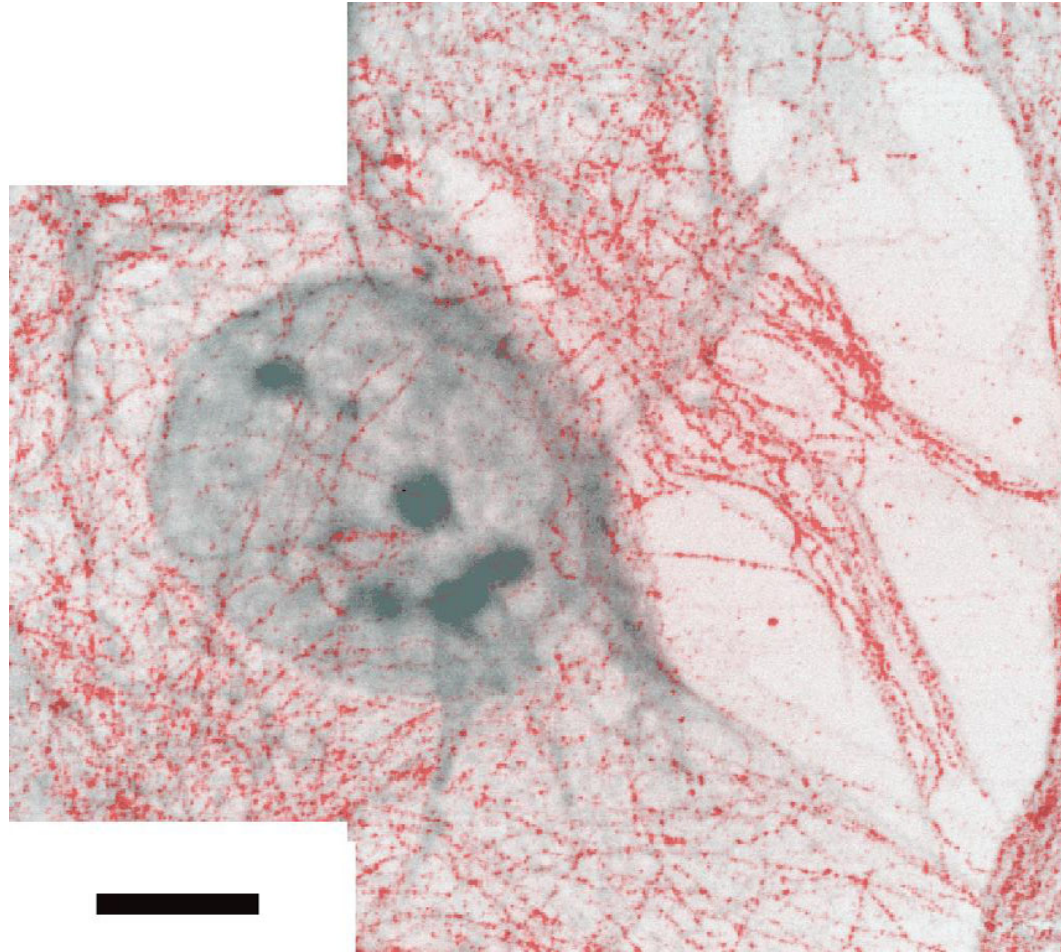
9 μm

Environmental/Earth Science 1994

diagenesis of coal



Gold labeled specimens 1996

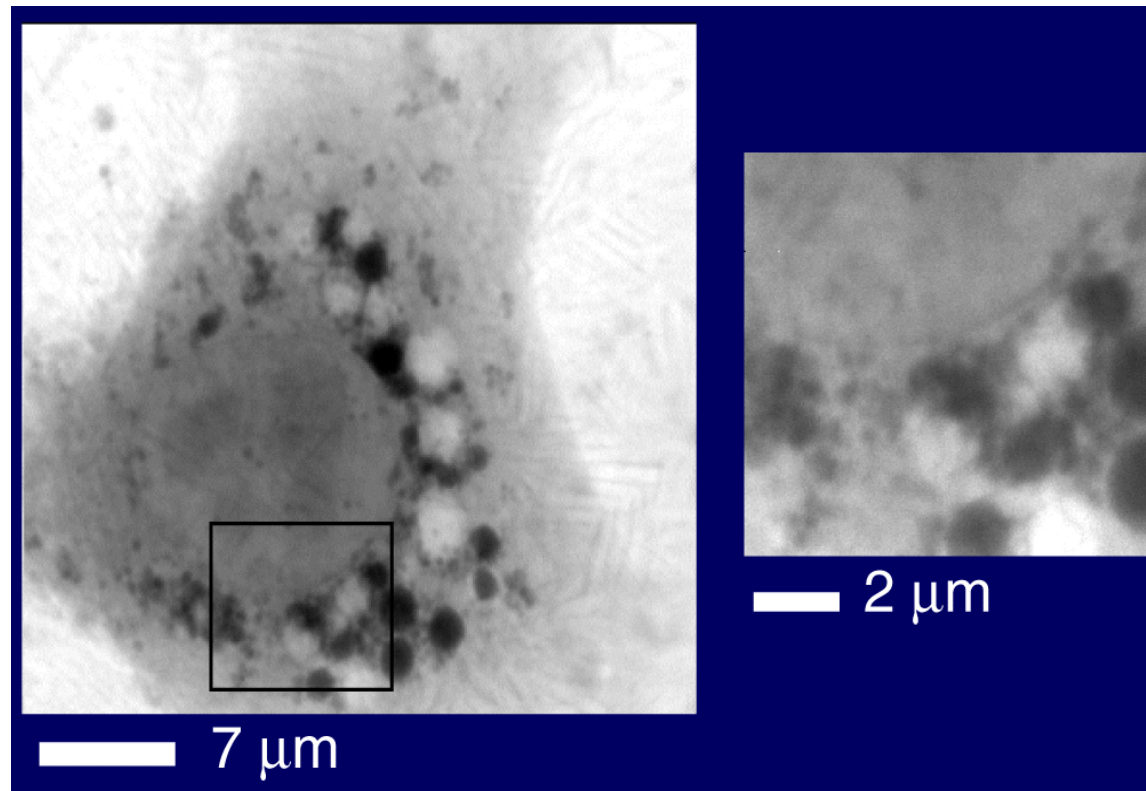


Chapman et al. J. Micr. Soc. Am
scale bar 7 microns

Cryo-STXM: Frozen-hydrated Fibroblasts 1999

Grids with live cells are

- Taken from culture medium and blotted
- Plunged into liquid ethane (cooled by liquid nitrogen)
- Loaded into cryo holder

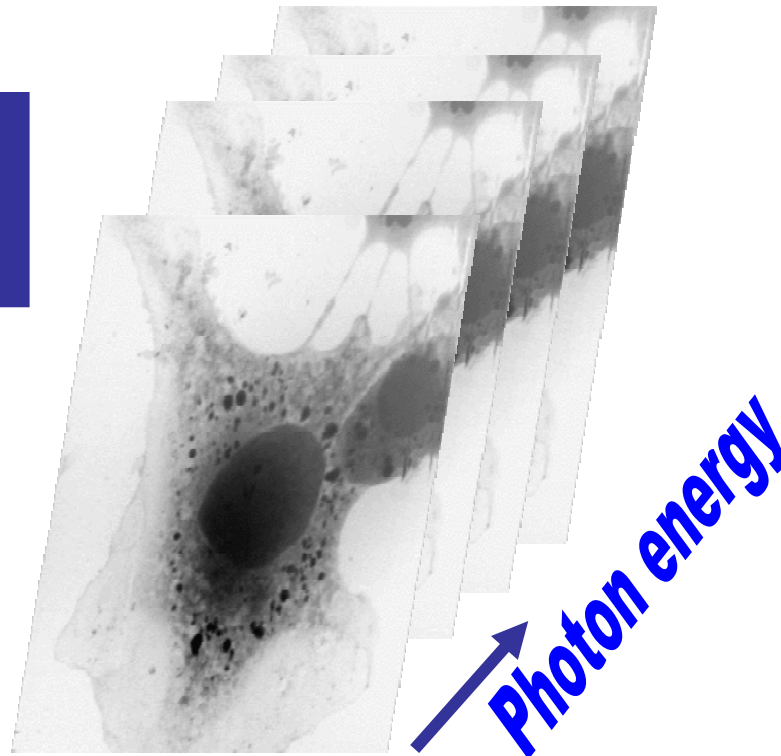


Spectromicroscopy by image stacks 1999

- Acquire sequence of images over XANES spectral region; automatically align using Fourier cross-correlations; extract spectra.

Images at $N=150$ energies are common.

IDL-based analysis tools are made available

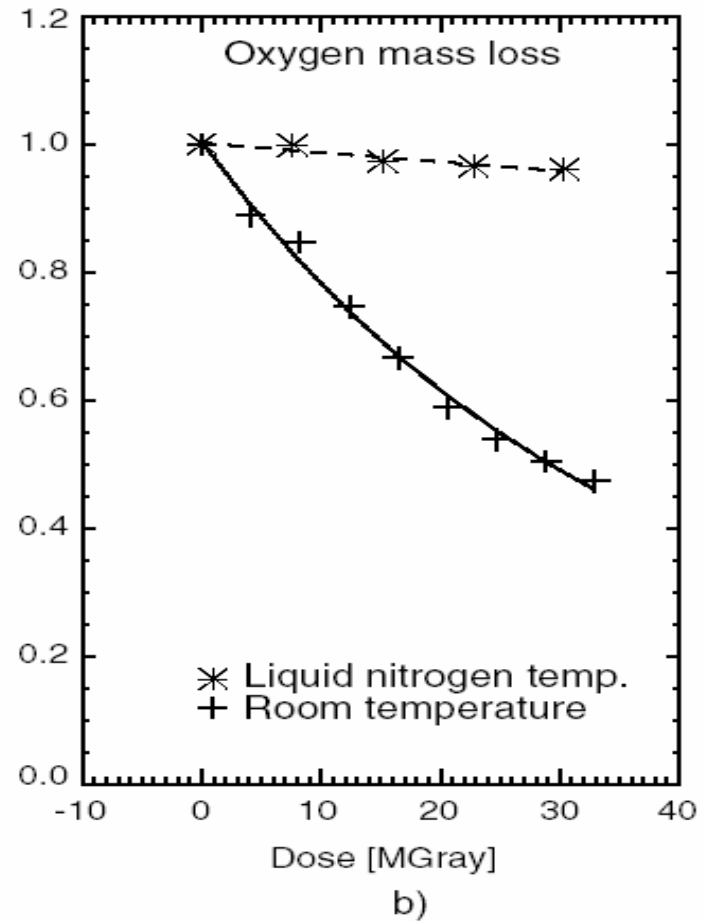
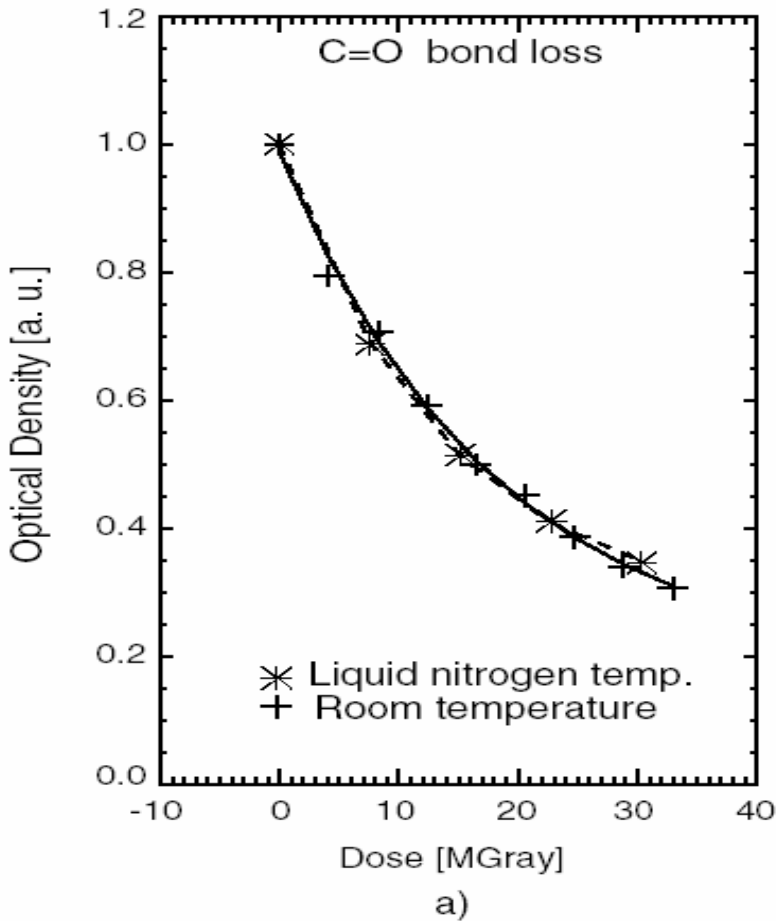


Analysis of stacks

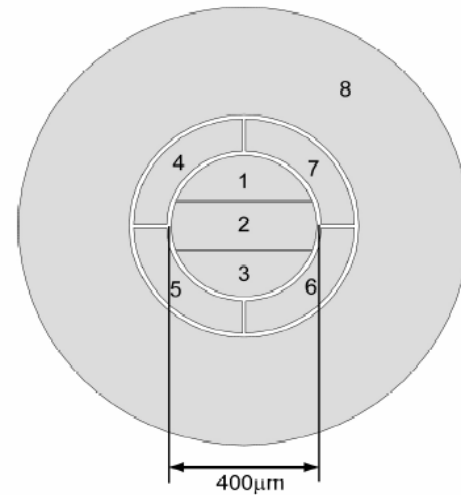
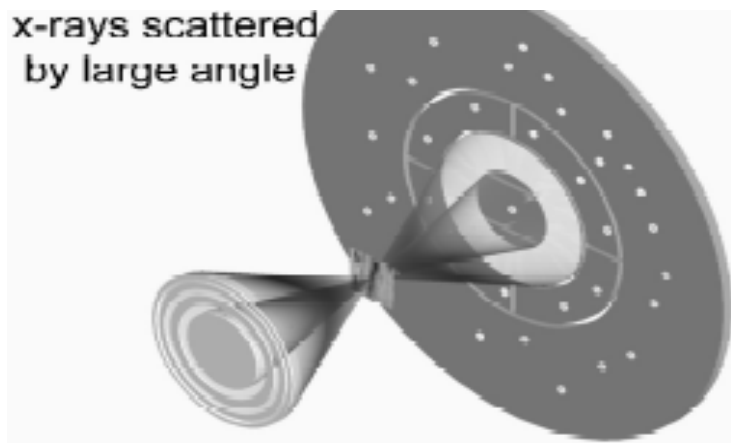
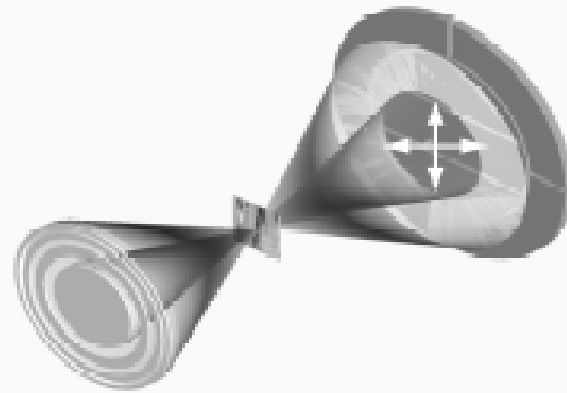
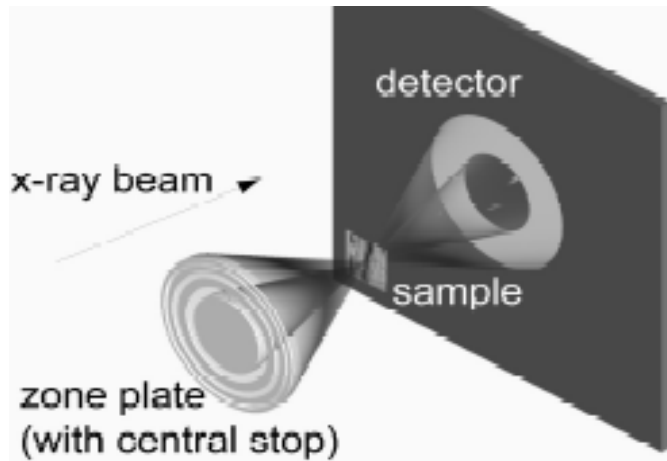
C. Jacobsen and students

- Singular Value Decomposition
 - (components and model spectra known)
- Principal Component Analysis
 - (components unknown)
- Cluster analysis

Cryo protects PMMA against mass loss, but not against chemical change!

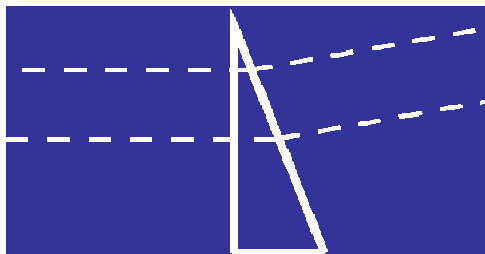


segmented detector 2001 (Stony Brook, BNL Instrumentation)

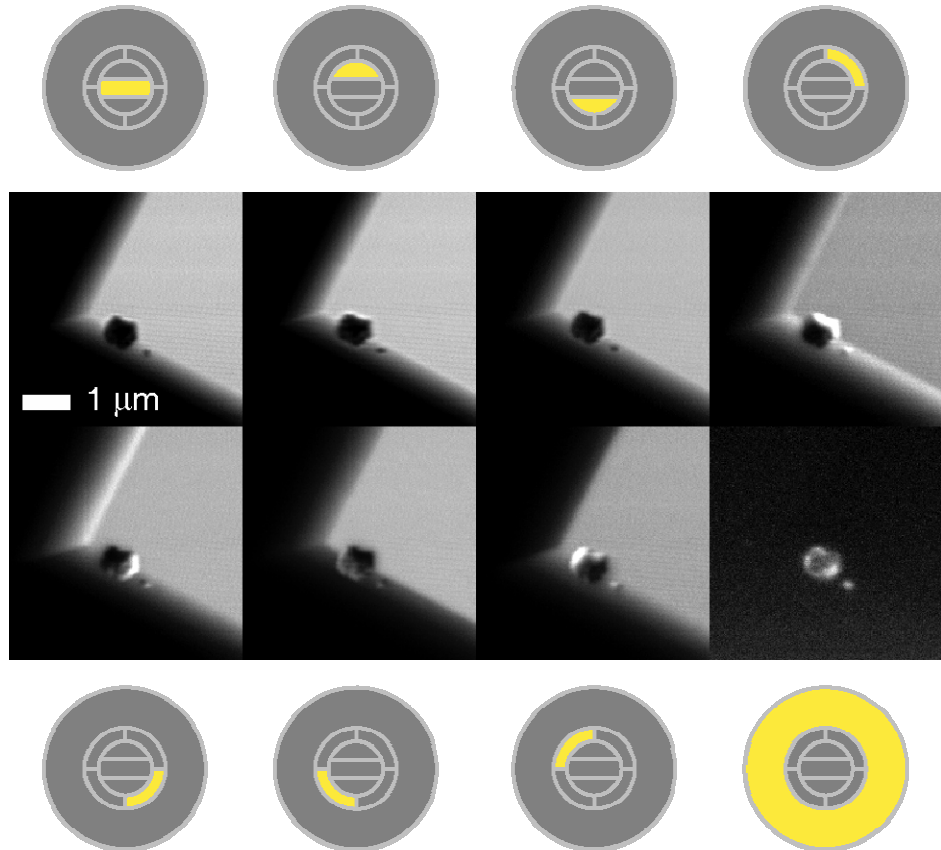


Segmented silicon drift detector

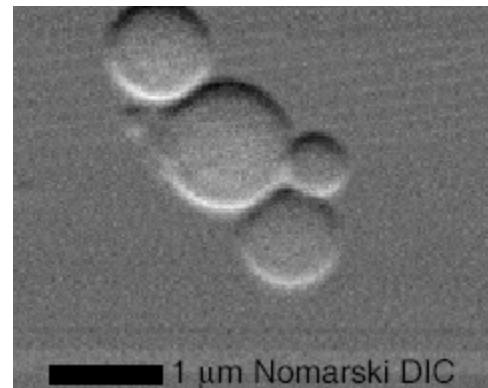
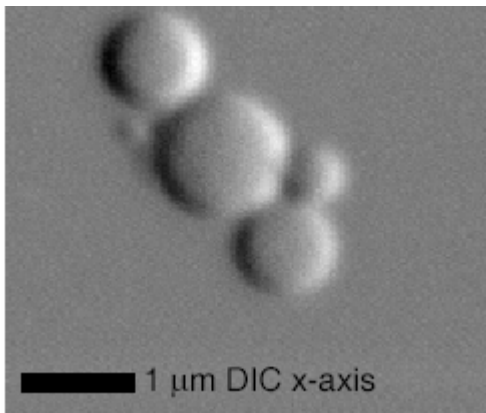
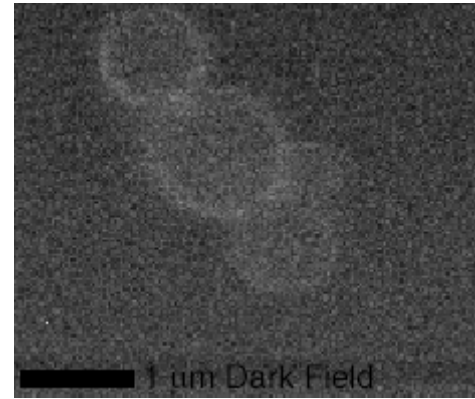
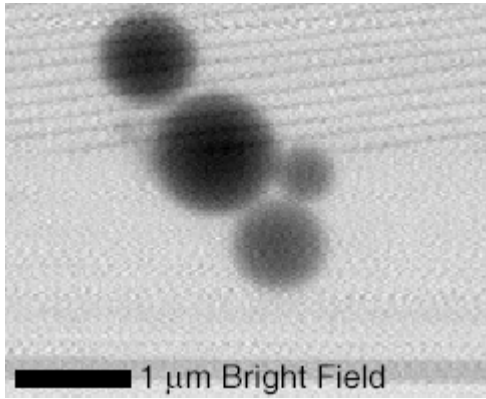
- Corner of silicon nitride window: silicon at $\sim 54^\circ$ wall slope forms a prism
- Refraction of x-ray beam in *opposite* direction from visible light prisms



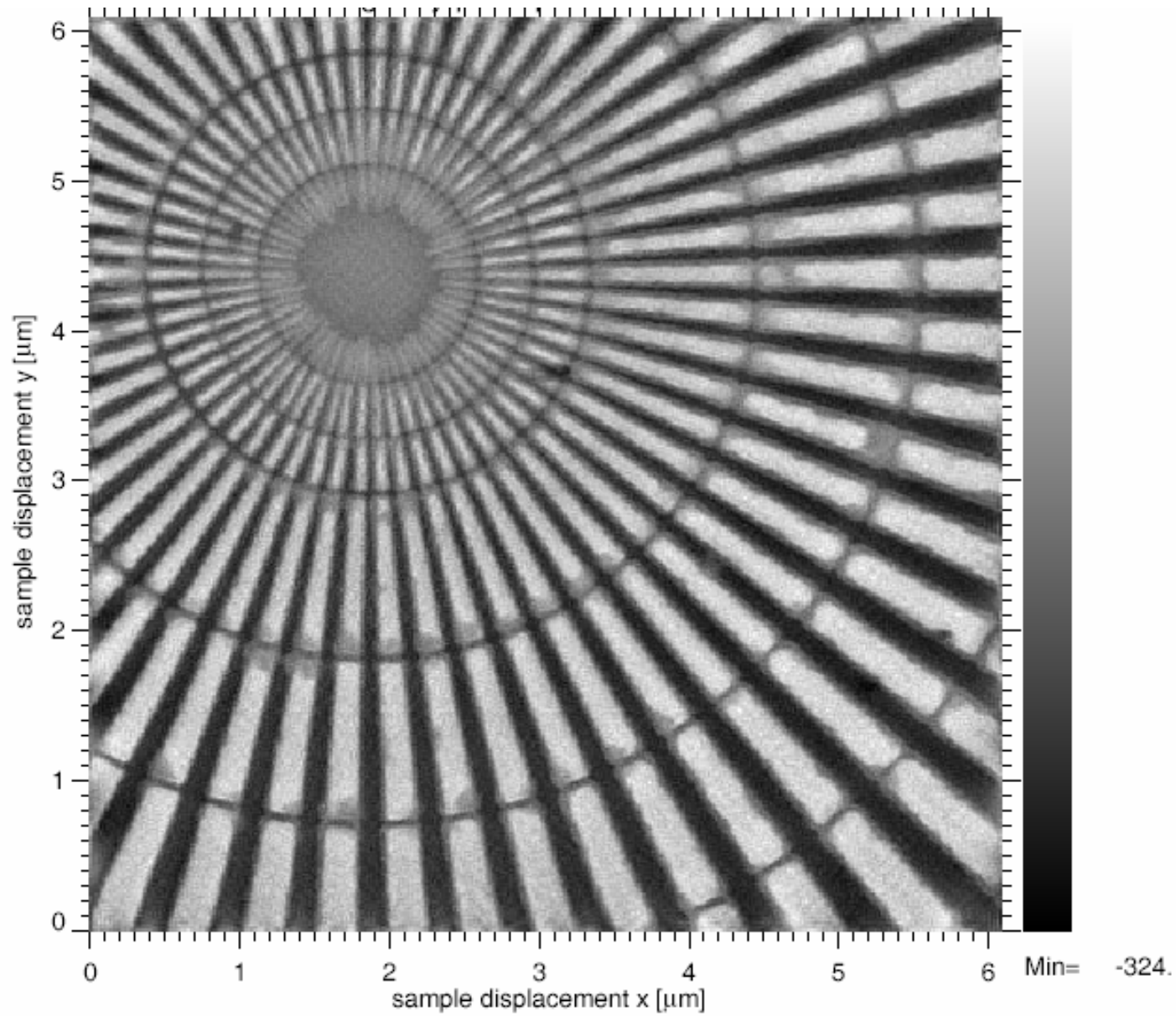
X-ray refractive index:
 $n = 1 - \delta - i\beta$



All channels acquired simultaneously



Feser thesis



Feser thesis

- Bright field: easy to make quantitative
- Phase contrast: edge enhancement,
good for high energy
- Dark field: emphasizes strong scatterers
- Luminescence: locates special labels
- Fluorescence: trace element sensitivity
(high energy)

STXM developments

Stony Brook / NSLS

- Zone plates 1983-'85 IBM
1987-'94: IBM/CXRO
1995- Bell Labs/SB
- Many students, postdocs, over the years:
 - Ade, Buckley, Chapman, Feser, Jacobsen, Kaznacheyev, Kenney, Ko, Lerotic, Lindaas, Maser, McNulty, Miao, Neuhäusler, Osanna, Rarback, Schäfer, Spector, Vogt, Wang, Winn, Yang, Yun, Zhang...

Stony Brook group today:

- Faculty: Chris Jacobsen, Janos Kirz
- Students: Holger Fleckenstein, Benjamin Hornberger, Bjorg Larsen, Enju Lima, Ming Lu, David Shapiro,
- Guest scientist: David Sayre
- Beamline scientist: Sue Wirick

Agere Inc.: Don Tennant

Many collaborators...

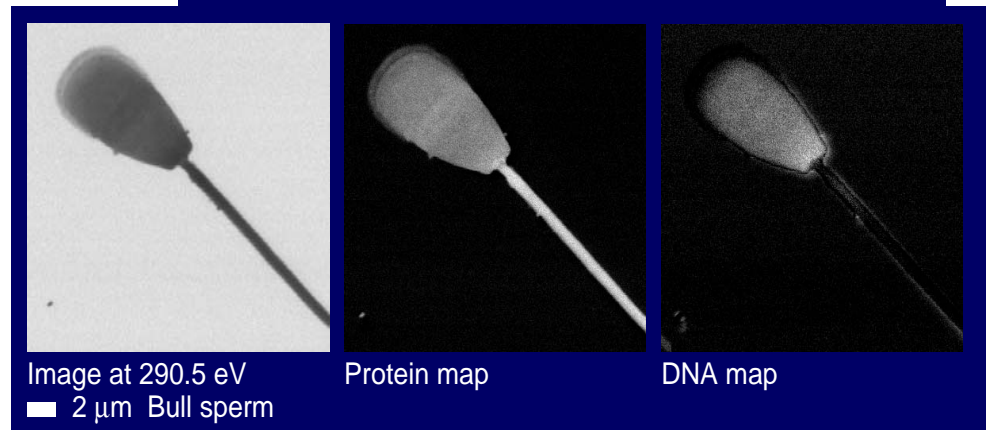
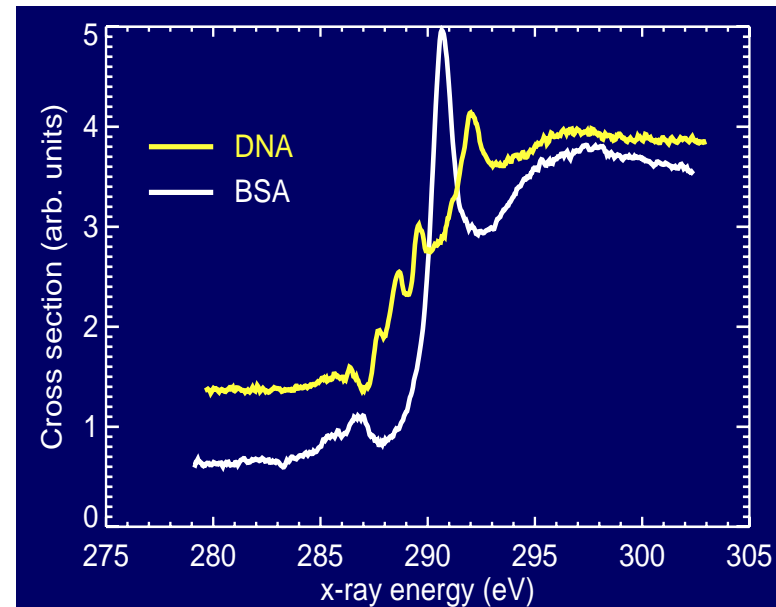
Applications @ NSLS X1A

- Sperm morphology / infertility Jacobsen, USB
- Interplanetary dust, meteoritics Flynn, SUNY/Plattsb.
- Organic geochemistry / wood, coal Cody, Carnegie Inst.
- Nuclear waste transport Schaefer, Karlsruhe
- Marine organic matter Brandes, U. Texas
- Bacteria and uranium chemistry Gillow, BNL
- Humic acid aggregates Rothe, Karlsruhe
- Humic and fulvic acids Scheinost, Zurich
- Biofilms Thieme, Goettingen
- Emulsion stability Urquhart, Saskatchewan
- PMMA: damage as fn of temp. Jacobsen, USB
-

DNA packing in sperm

- X. Zhang, R. Balhorn, J. Mazrimas, and J. Kirz, *J. Structural Biology* **116**, 335 (1996)
- DNA packing in sperm mediated by protamine I and protamine II; fraction of protamine II can vary from 0% to 67% among several species
- Bulk measurements: compromised by immature or arrested spermatids
- Conclusion: protamine II replaces protamine I, rather than binding to protamine I complex

5/8/2006



Air-dried bull sperm

Sperm morphology and infertility



■ 2 microns

- Study to shed light on correlations of morphology, and biochemistry, in male infertility
- Image of wet, unfixed human sperm

STXM / Spectromicroscopy today

- ALS:

Polymer STXM - 5.3.2

- Interferometric stage control
(NCSU/ALS/McMaster team 2001)

MES STXM - 11.0.2

- NSLS: STXM IV, CRYO, (STXM V)
- Elsewhere: ESRF, APS, Hsinchu
BESSY II, (CLS), (SLS),...

NC STATE UNIVERSITY

McMaster University

DOW
Living. Improved daily.

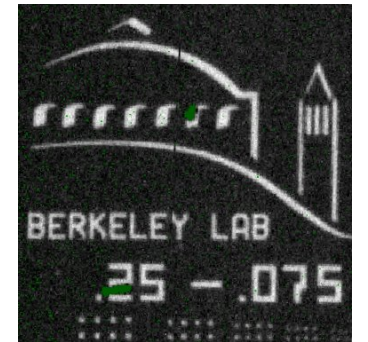
STONY BROOK
STATE UNIVERSITY OF NEW YORK

L·B·N·L
Advanced Light Source



5.3.2 Polymer STXM: First Tests

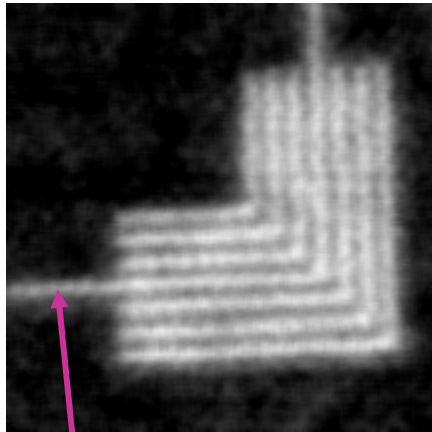
A.L.D. Kilcoyne, T. Tyliszczak, M. Kitcher, Peter Hitchcock, S. Fakra, K. Frank, C. Zimba, M. Rafailovich, J. Sokolov, G. Cody, E. Rightor, G. Mitchell, I. Koprinarov, E. Anderson, B. Harteneck, Adam Hitchcock, T. Warwick, H. Ade



Polymer STXM image of test pattern

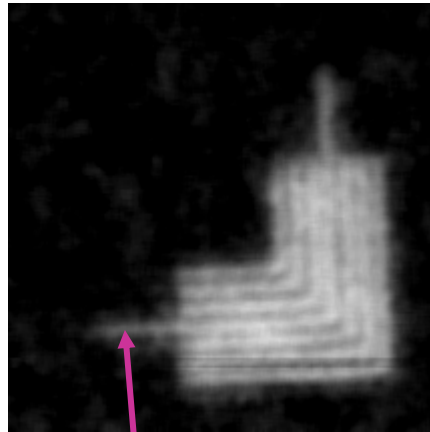
CXRO test-pattern imaged at 390 eV

Resolved 40 nm
1:1 features



Isolated 40 nm line

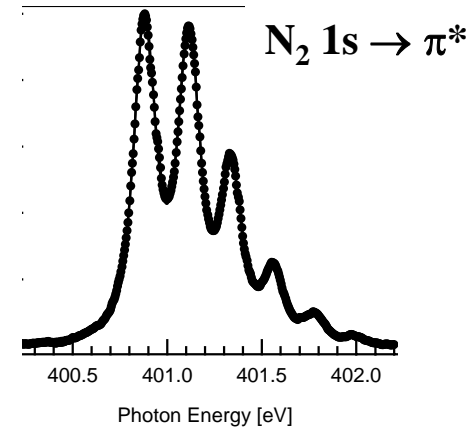
Resolved 30 nm
1:1 features



Isolated 30 nm line

Experiments: T. Tyliszczak, H. Ade, D. Kilcoyne

Excellent, stable flux: > 1 MHz
Excellent energy resolution: <60 meV

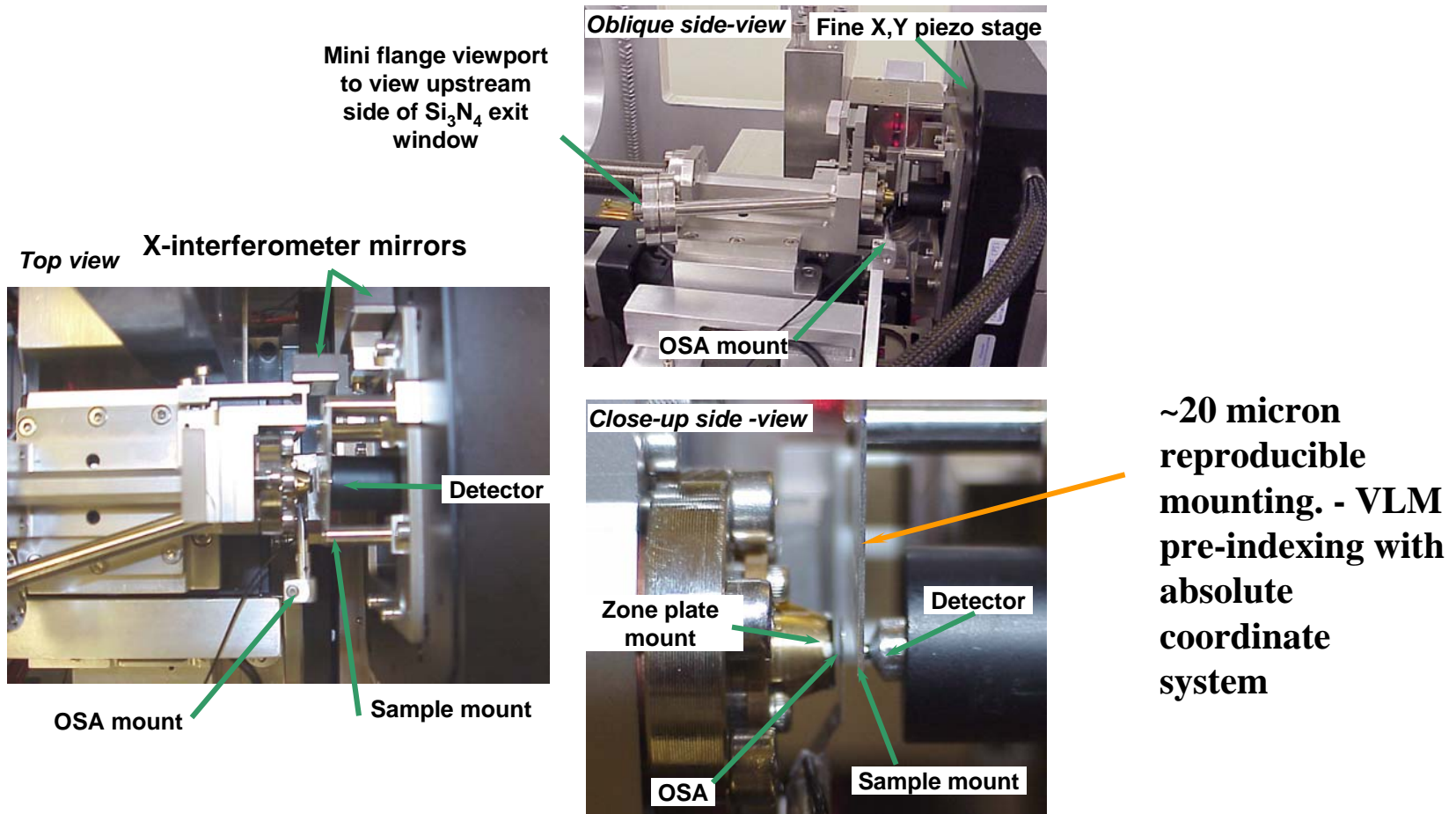


Some improvements still ahead

Supported by NSF DMR-9975694, DOE DE-FG02-98-ER45737
Dow Chemical and NSERC

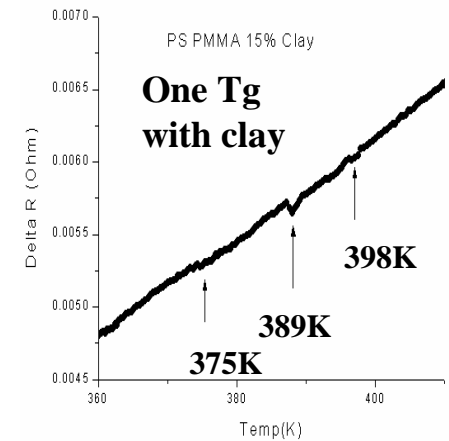
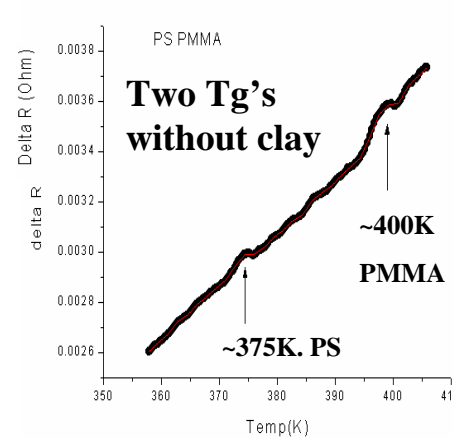
First 5.3.2 STXM Results
ALS News Fall 2001.ppt

Some close-up views of 5.3.2 hardware



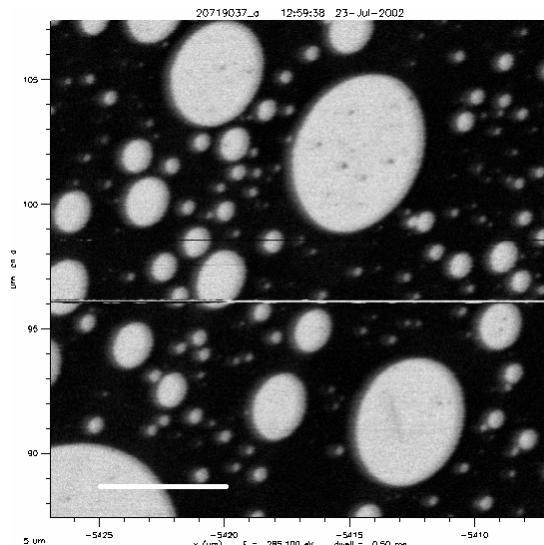
Polymer Clay Composites: PS/PMMA

- Clay works better than copolymer to “compatibilize” the blend
- Observe the same in bi-layer geometry

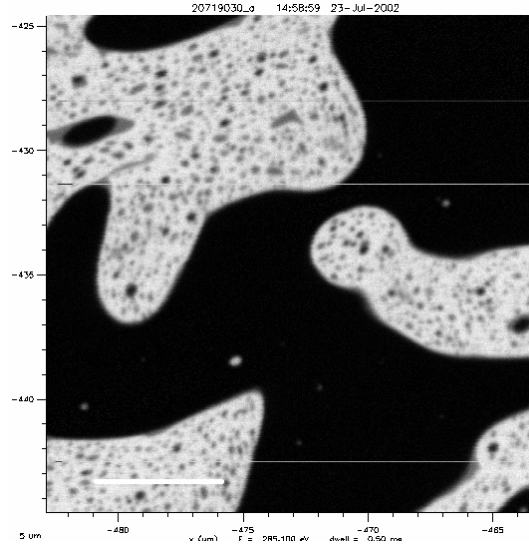


DSC suggest formation of “single” phase in the presence of clay

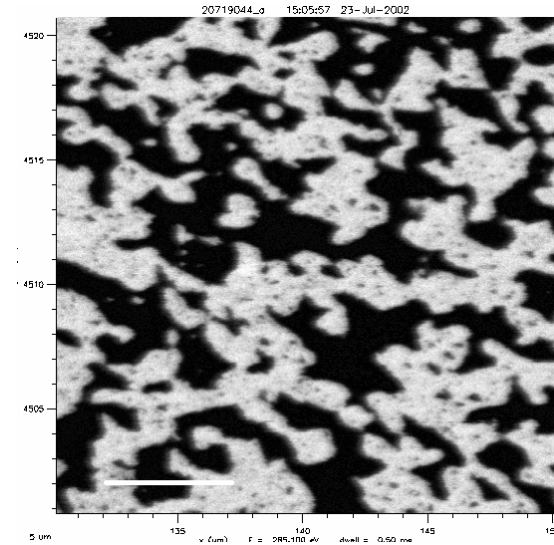
PS/PMMA 70/30



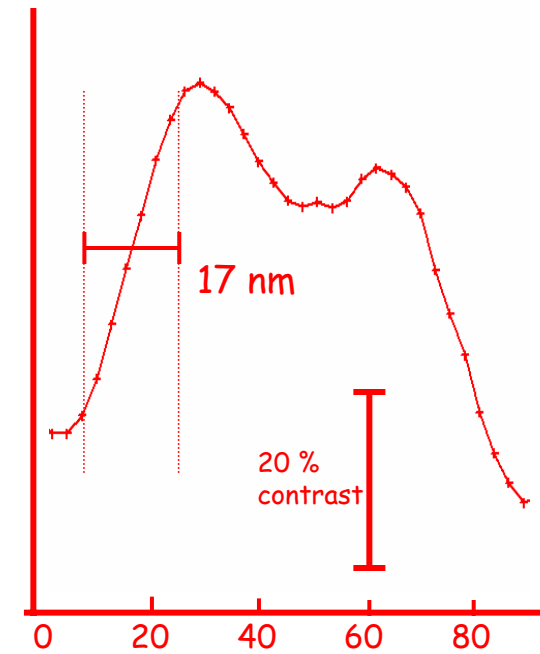
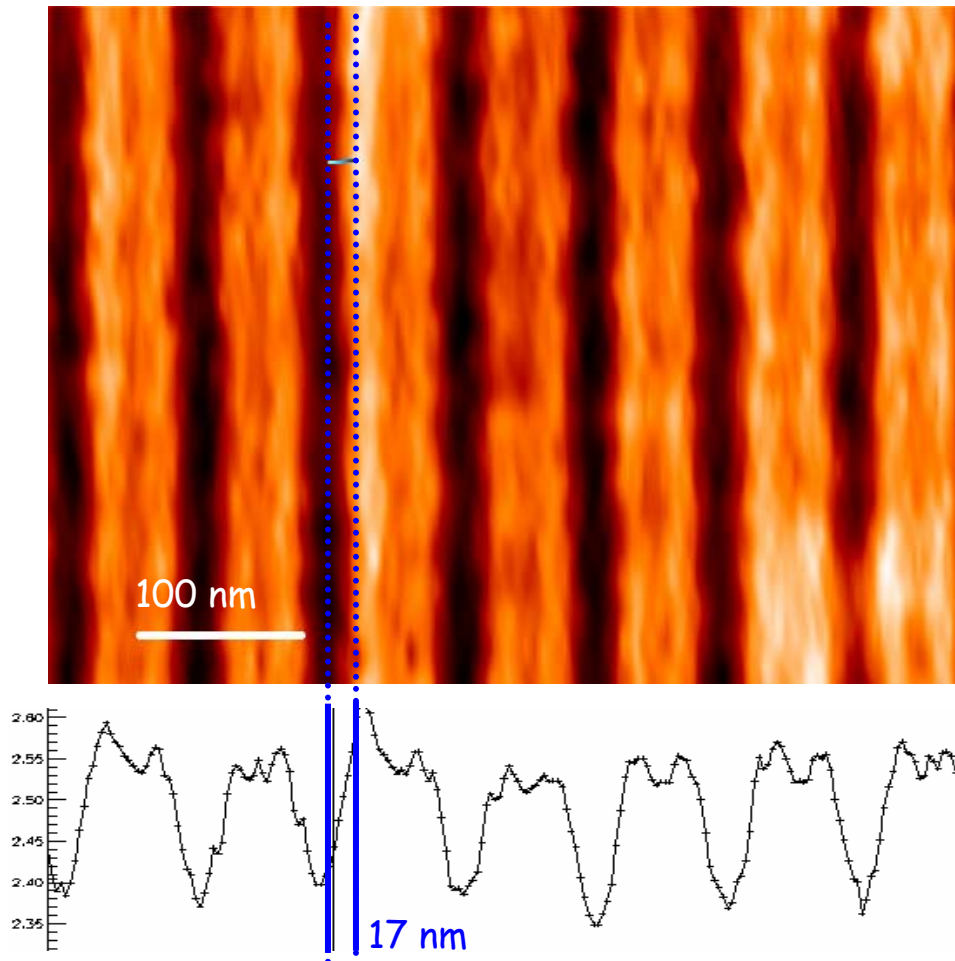
PS/PMMA/P(S-c-MMA) 45/45/10



PS/PMMA/Clay 45/45/10

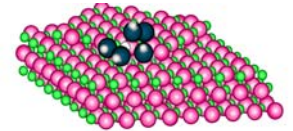


Very good Resolution with 25 nm zone plate

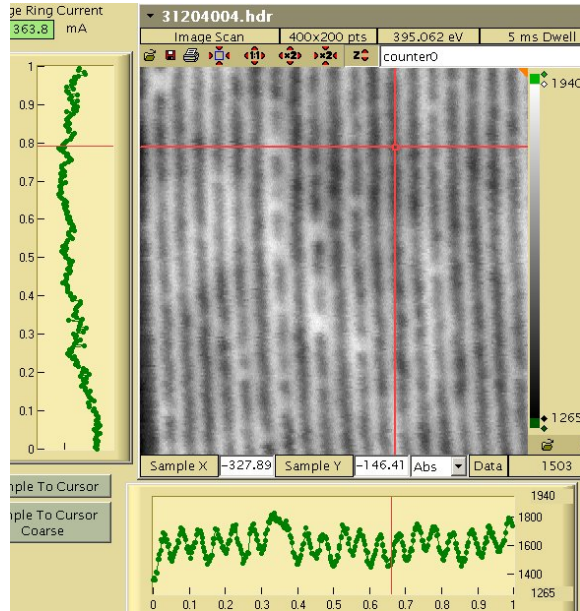


Scanning transmission x-ray microscope image of a 25 nm test pattern (1:2 spacing)

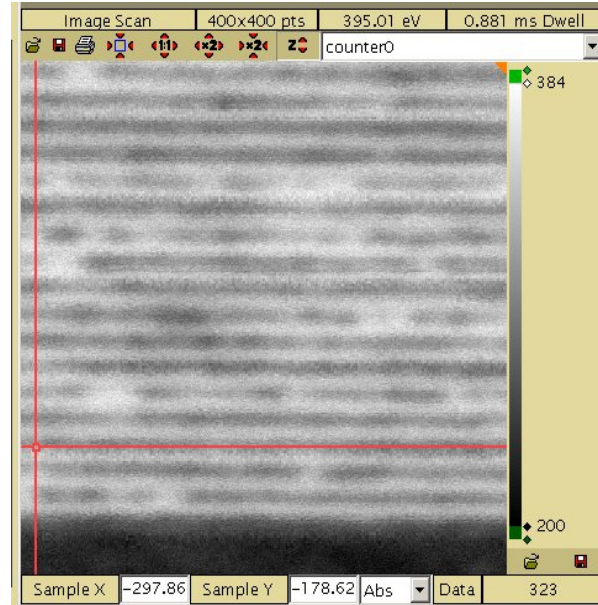
Images of 25 nm test pattern



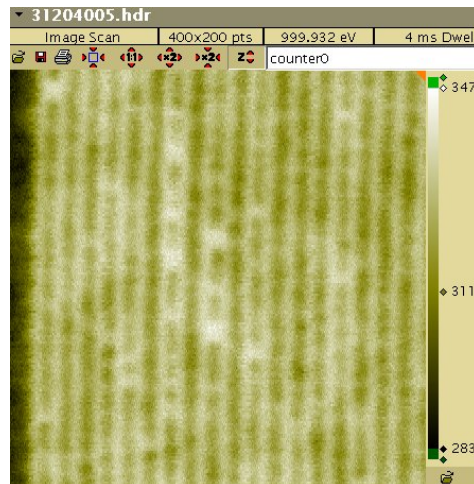
ALS-MES 11.0.2



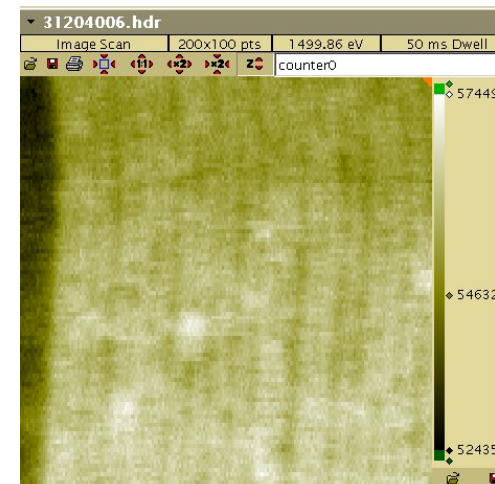
395eV



600eV



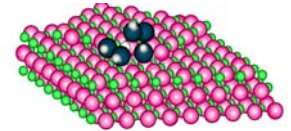
1000eV



1500eV



Current ALS-MES STXM Status



ALS-MES 11.0.2

- Energy range: 80 eV – 2100 eV – energy resolution > 7500
- Spot size: 30 nm (theoretical)
- Can resolve smaller structures (15 nm)
- Photon flux: up to 10^9 ph/s with full spatial resolution and energy resolving power > 3000
- Resolution limited by the zone plate
- 4 basic zone plates: 25 nm and 35 nm , 40 nm and 45
- Maximum scanning rate: 12 Hz
- Scanning range: 4000x2000 pixels – up to 20 x 4 mm
- Minimum step size 2.5 nm
- Precision of staying at the same spot for spectra acquisition:
 - < 50 nm (laser interferometry)
- EPU – polarization dependence, circular dichroism + electromagnet
- Possibility to scan sample at 30 deg to the beam – out of plane polarization, in plane magnetization
- Single photon timing capabilities (100 ps)

Scanning Transmission X-ray Microscopy Study of Microbial Calcification

Microbes are often associated with calcium-containing minerals in nature, but it is difficult to determine if these organisms are involved in mineral nucleation: search for biosignatures in fossilized microbial cells.

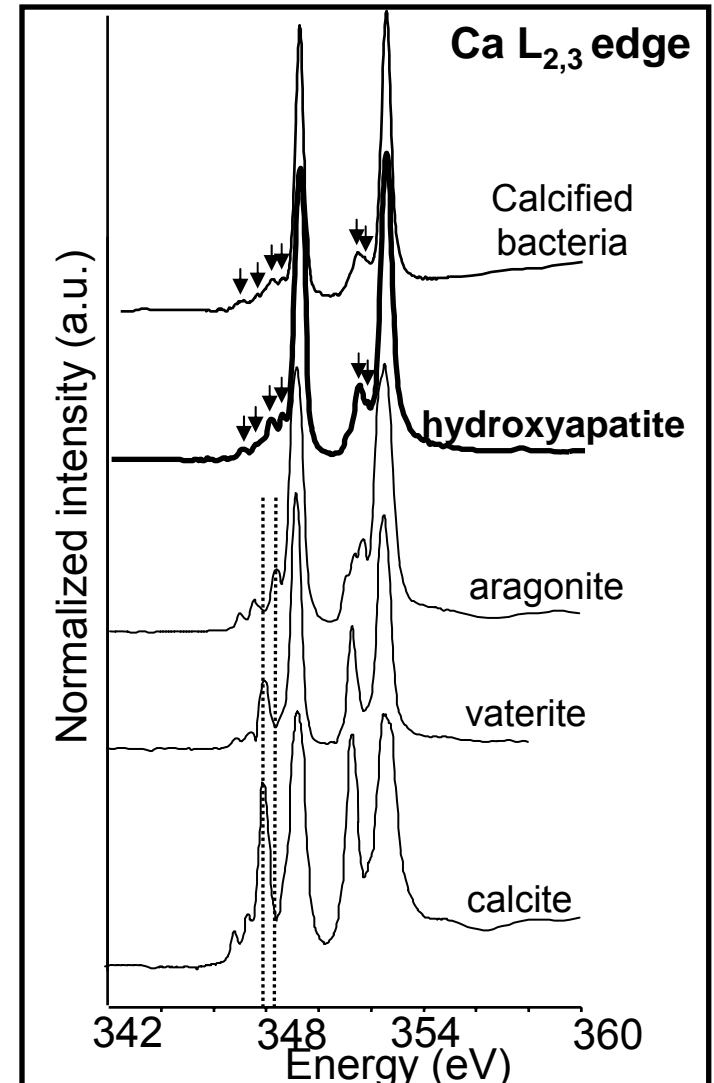
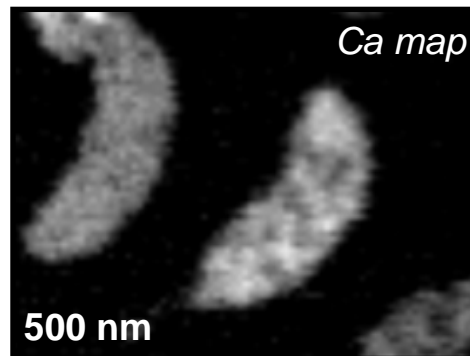
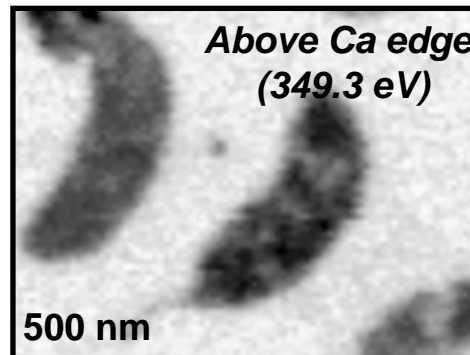
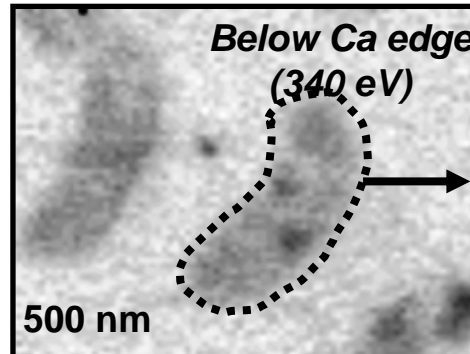
Experiment:

STXM used to obtain NEXAFS spectra at the C K-edge and the Ca L_{2,3}-edge on both the minerals and associated organics during biomineralization by *Caulobacter crescentus* cells under laboratory conditions.

Results:

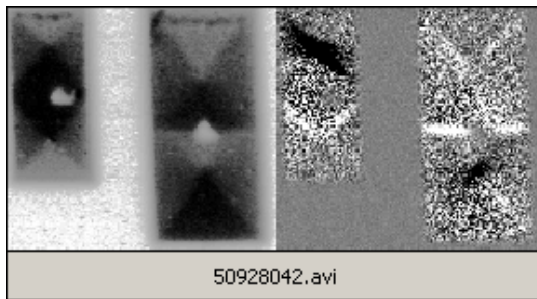
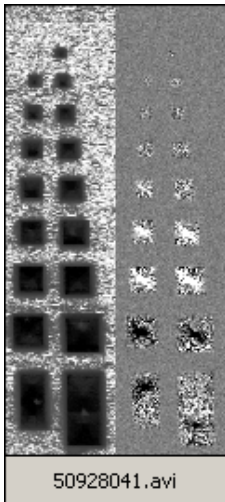
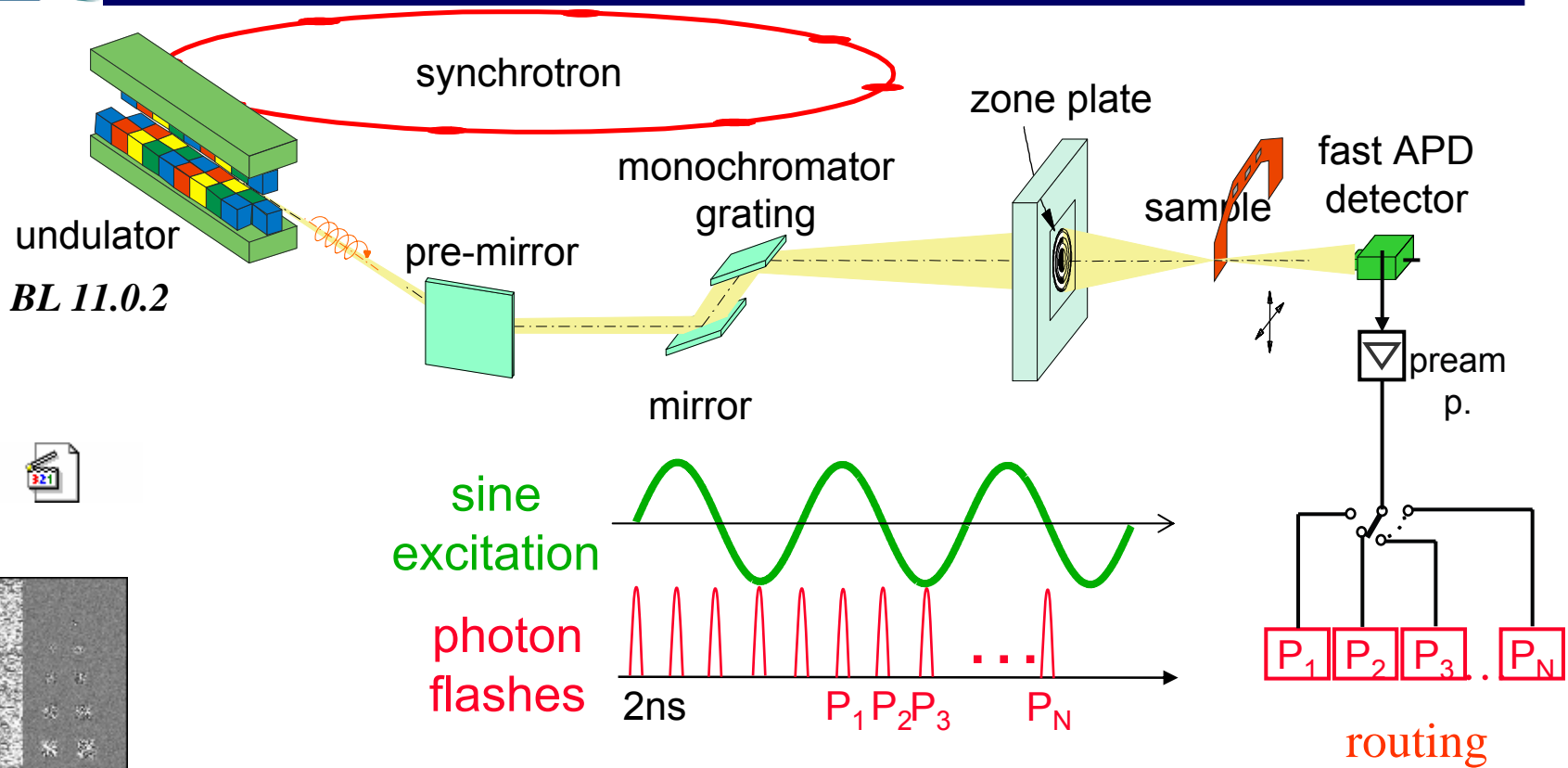
Ca L_{2,3}-edges for hydroxyapatite, calcite, vaterite, and aragonite are unique and can be used as probes to detect these different mineral phases.

C. crescentus cells, when cultured in the presence of high calcium concentration, precipitate carbonate hydroxyapatite.

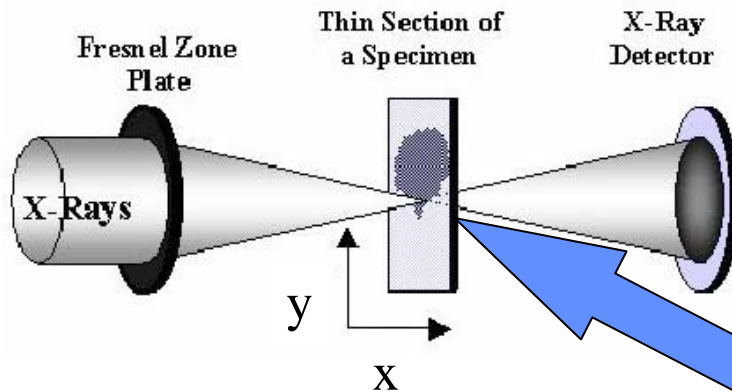


K. Benzerara, T.H. Yoon, T. Tyliczszak, B. Constantz, A.M. Spormann, and G. E. Brown, Jr. *Geobiology*

Time-Resolved STXM Magnetic Measurements in multi-bunch mode



A. Puzic, B. Van Waeyenberge, K.W. Chou, P. Fischer, H. Stoll, G. Schütz, T. Tyliczszak, K. Rott, H. Brückl, G. Reiss, I. Neudecker, T. Haug, M. Buess, C.H. Back, „Spatially Resolved Ferromagnetic Resonance: Imaging of ferromagnetic eigenmodes“ J. Appl. Phys. 97 10E704 (2005). LBNL-56923

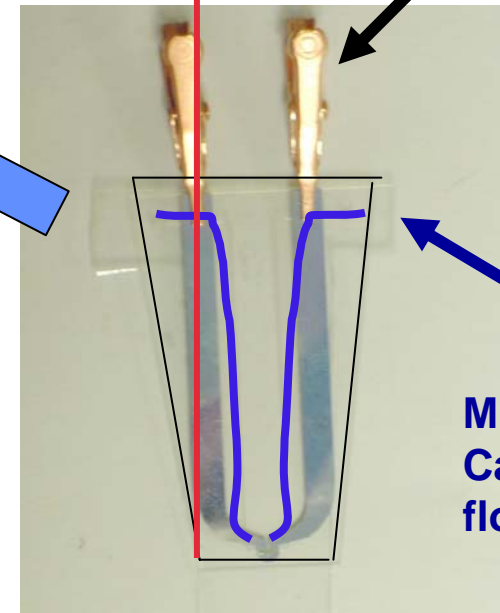


Data Acquisition

- Flow Switching
- Pressure
- Temperature Control

Thermocouple

Resistive heater



Sandwich two silicon nitride windows around this holder to create gas cell



Sample is placed on one of the windows

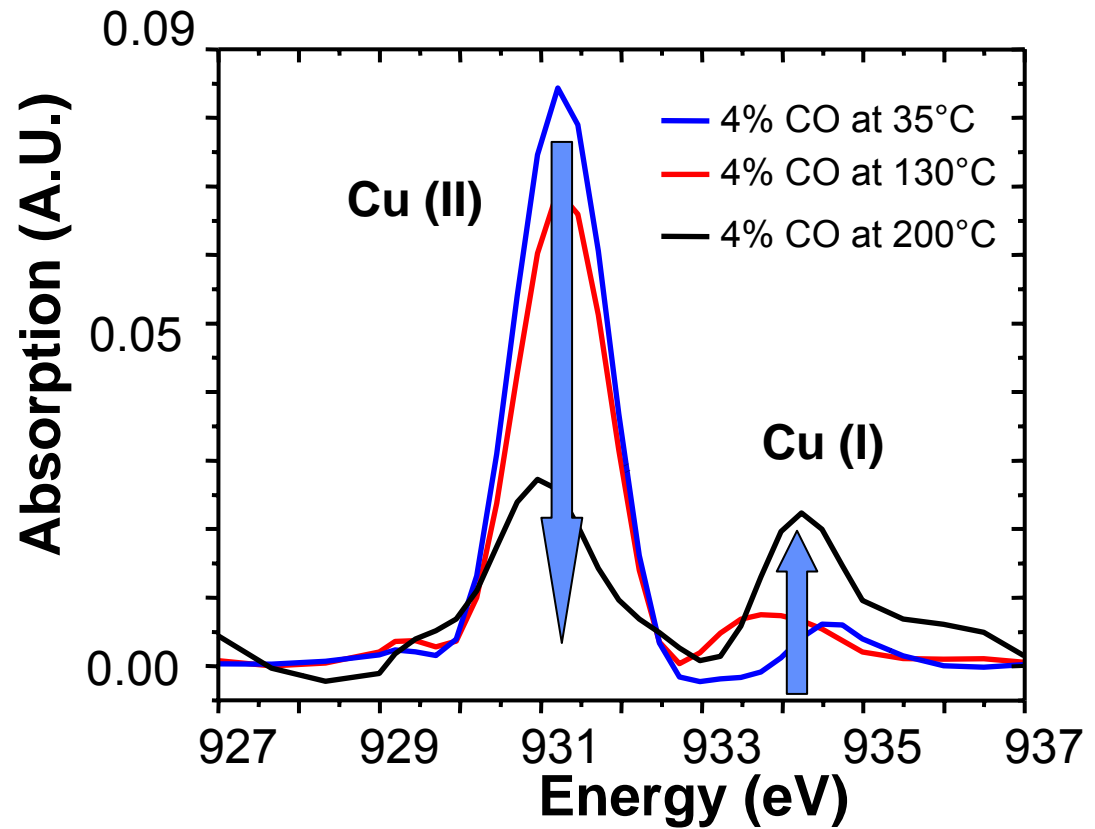
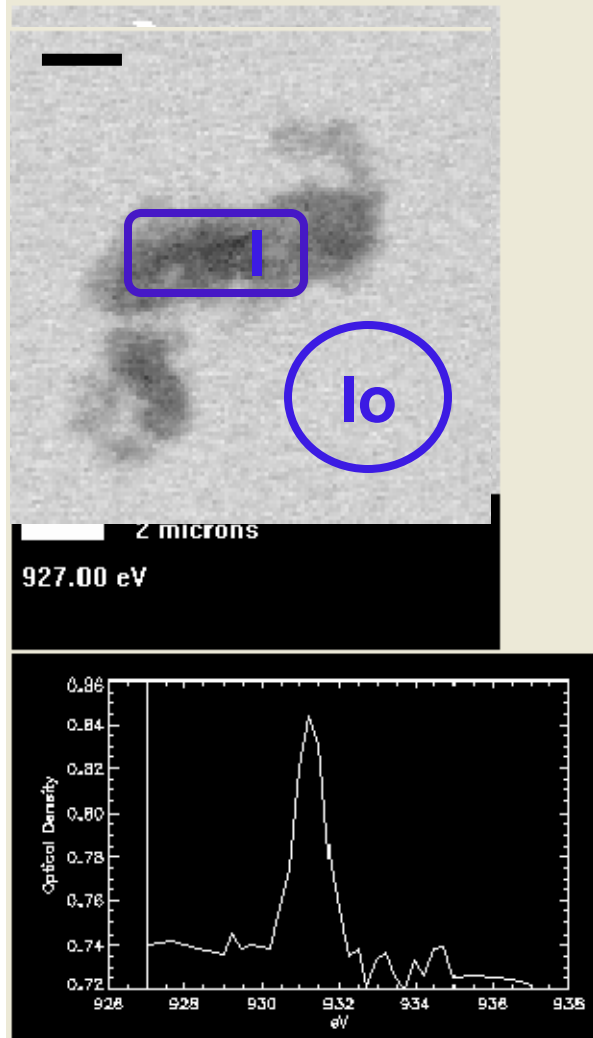
Applications

Soot oxidation and subsequent particle growth

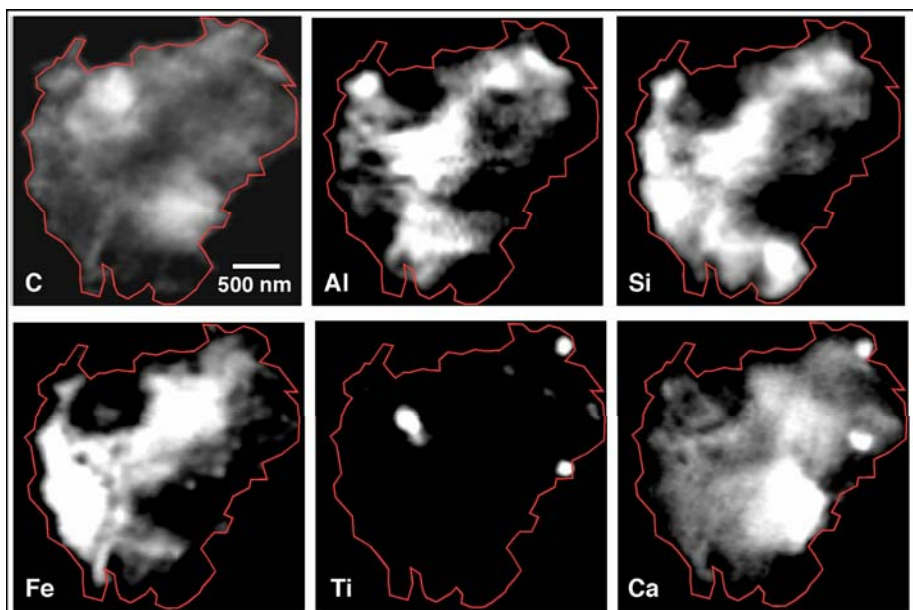
Catalysis

Water uptake on patterned photo resists

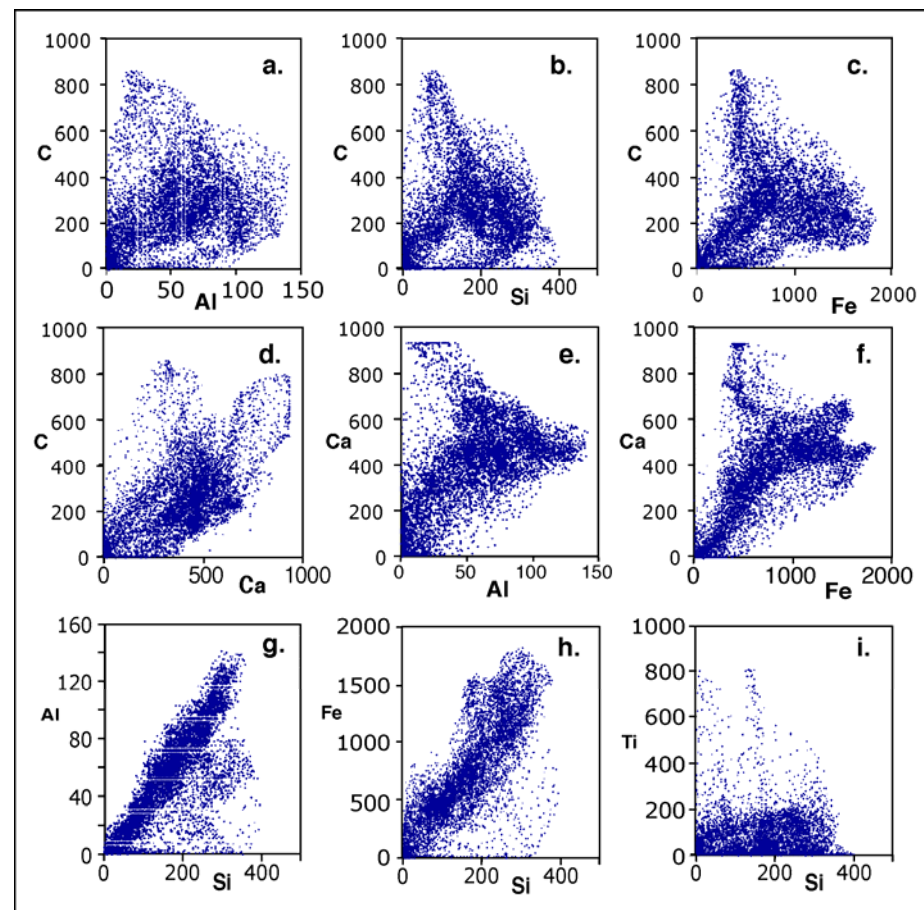
I. Drake, T.C. N. Liu, M. K. Gilles, T. Tyliszczak, A.L.D. Kilcoyne, D.K. Shuh, R.A. Mathies, and A.T. Bell
 "Micro reactor for in-situ Transmission Soft X-ray Absorption Studies of Supported Catalysts and Environmental Materials." Rev. Sci. Inst. 75(10) 3242-3247 (2004).



Monitor changes on a single particle during oxidation and reduction



C – “organic” carbon (map at 288.3 eV)

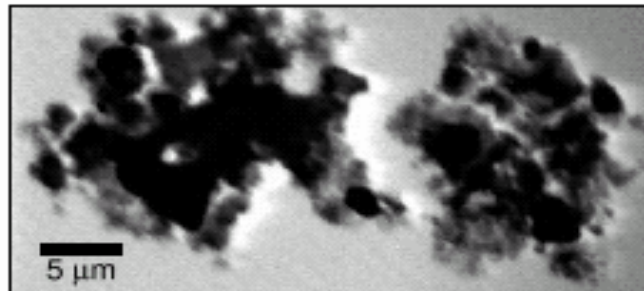


Correlation plots of net counts (arbitrary units) obtained from STXM maps. Both maps and plots are based on 30 nm pixels over a $9 \mu\text{m}^2$ area (10^4 pixels).

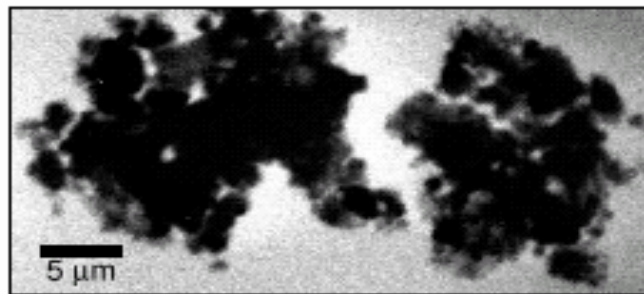
J. Wan, T. Takunaga, T. Tyliszczak, LBNL

STXM @ BESSY II

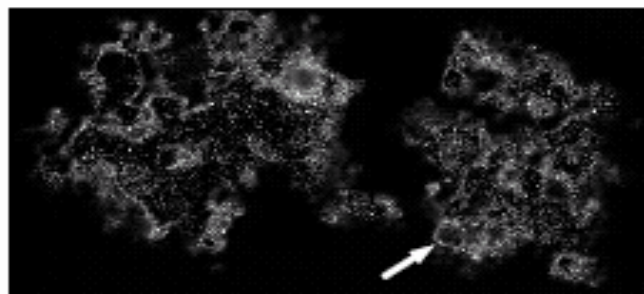
Urs Wiesemann thesis, 2003



280 eV

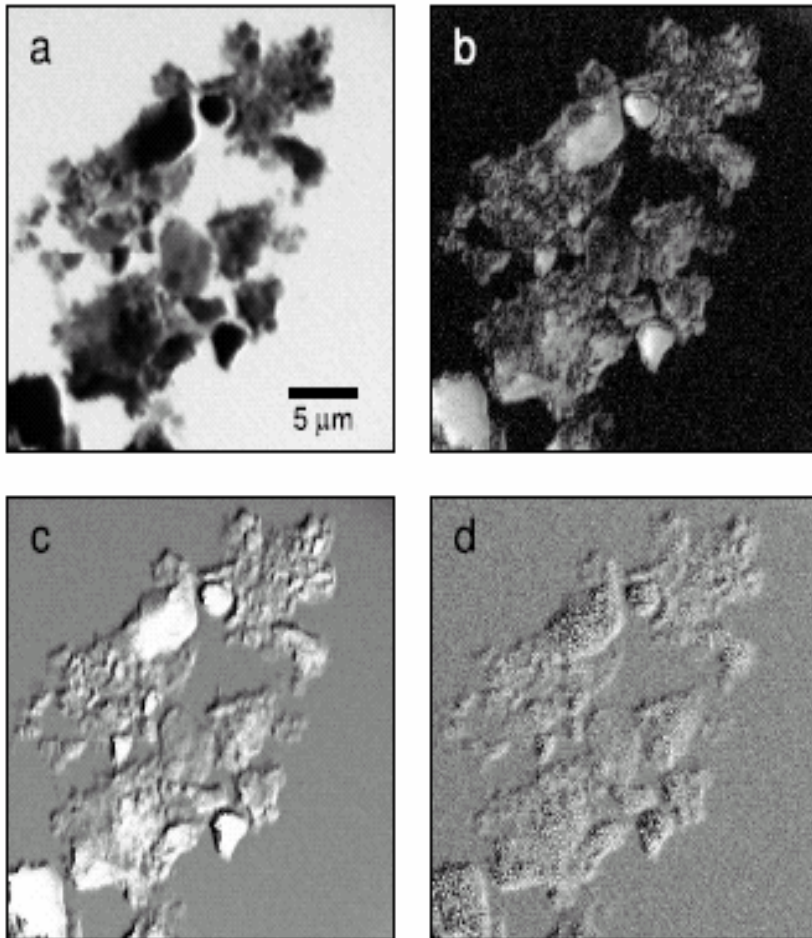


292 eV



Elemental imaging at the carbon absorption edge of two flocks of Colloidal particles from a chernozem soil in dry state on a silicon membrane. Shown are the absorption contrast images below the absorption edge at 280 eV (I11, top), above the absorption edge at 292 eV (I12, center), and the carbon mass density m_C calculated using Eq. (6.1) (bottom). The arrow in the mass density image indicates an organically coated particle. The images have 400×200 pixels of $100 \times 100 \mu\text{m}^2$ size; the pixel dwell time is 6ms.

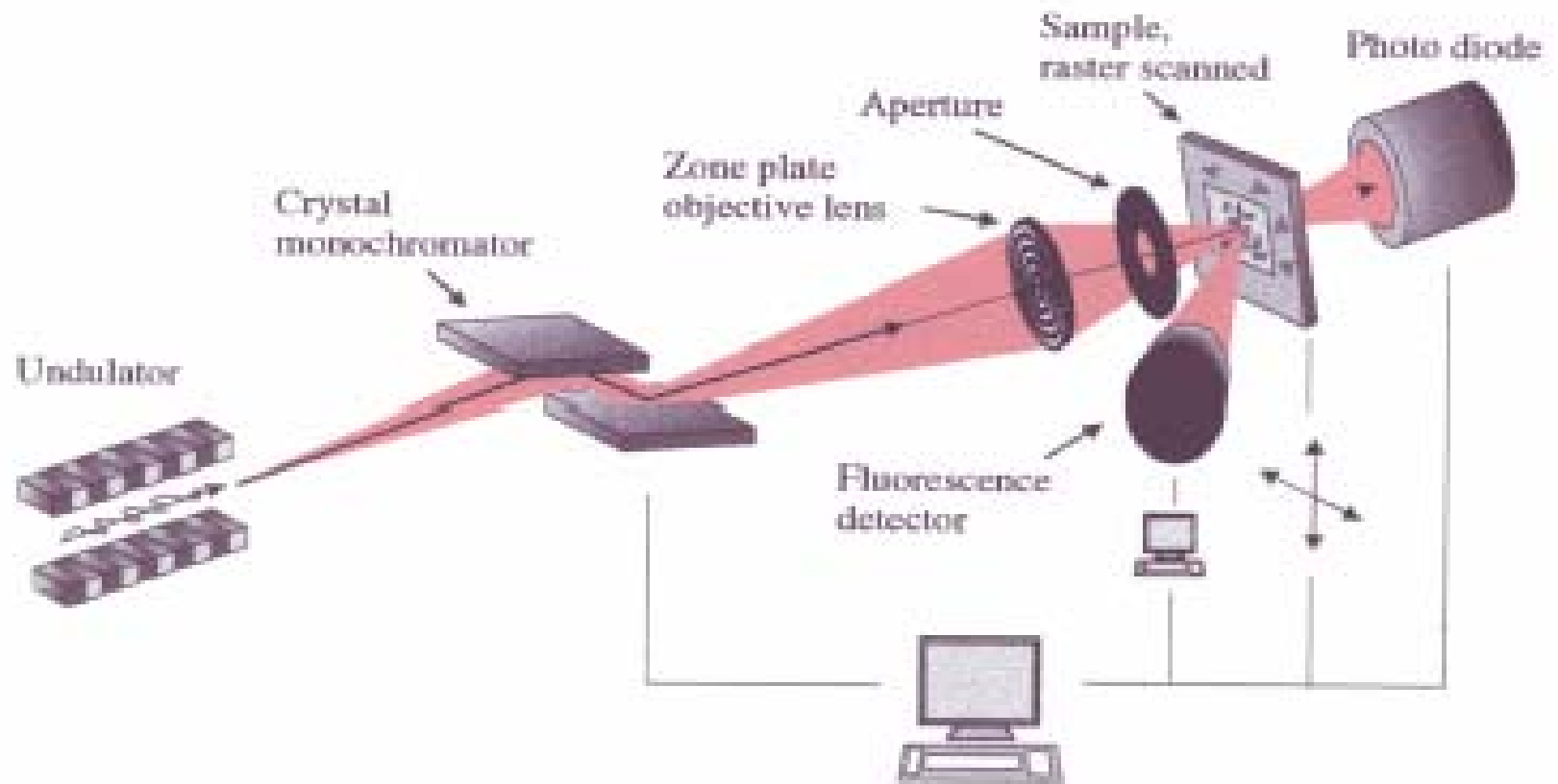
Urs Wiesemann thesis



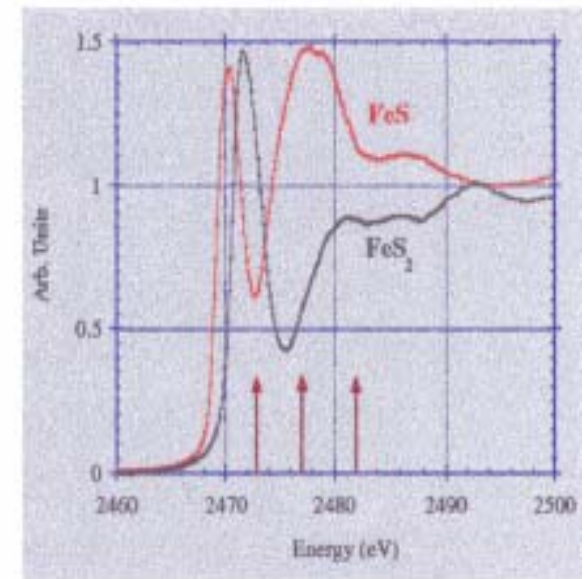
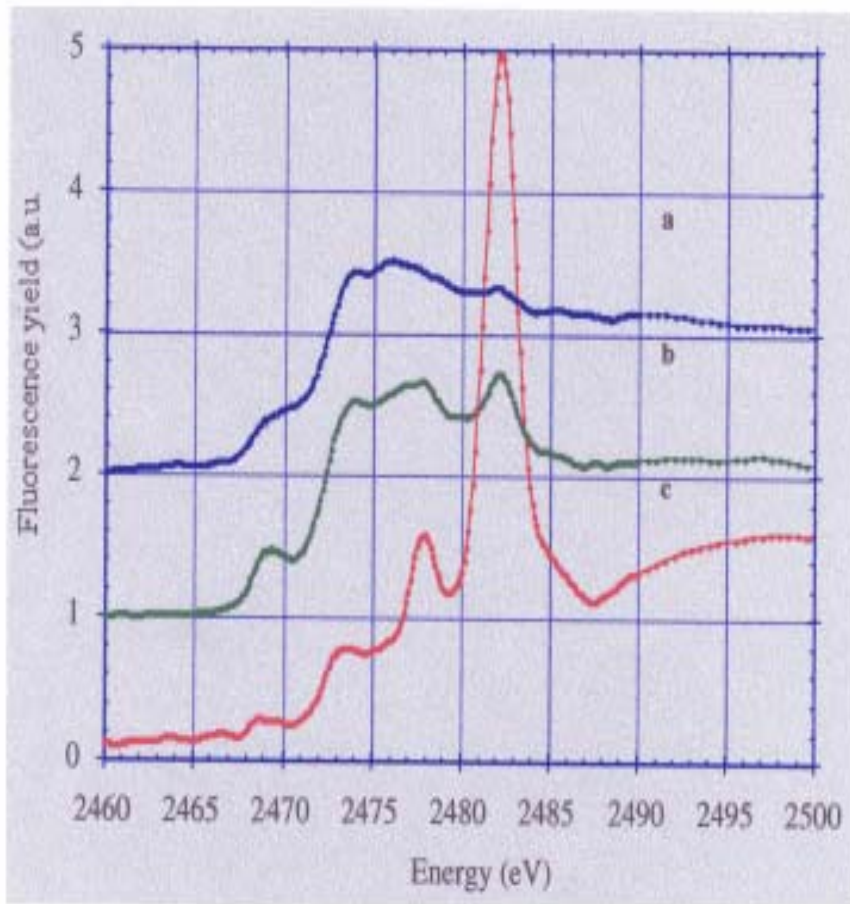
Colloidal particles from a chernozem soil in dry state on silicon membrane imaged in incoherent bright field and differential phase contrast.

(a) Incoherent bright field contrast; (c) differential phase contrast in horizontal direction; (d) differential phase contrast in vertical direction; (b) square root of the quadratic sum of the horizontal and vertical phase contrast images (bottom). All images are generated from a single scan of 400×400 pixels with a step size is 75nm and 6ms dwell time; the photon energy is 408 eV.

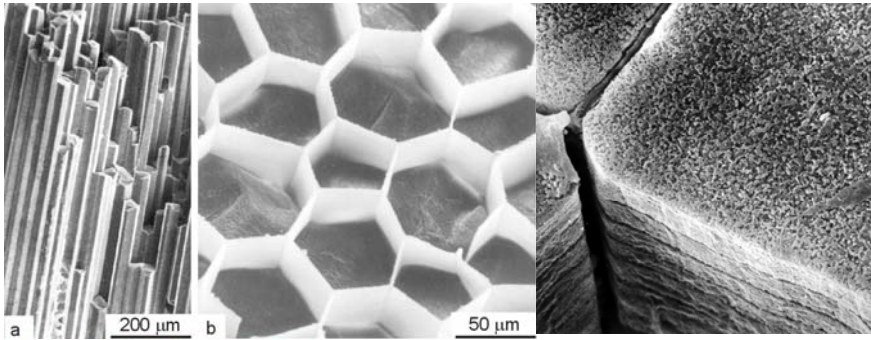
ESRF



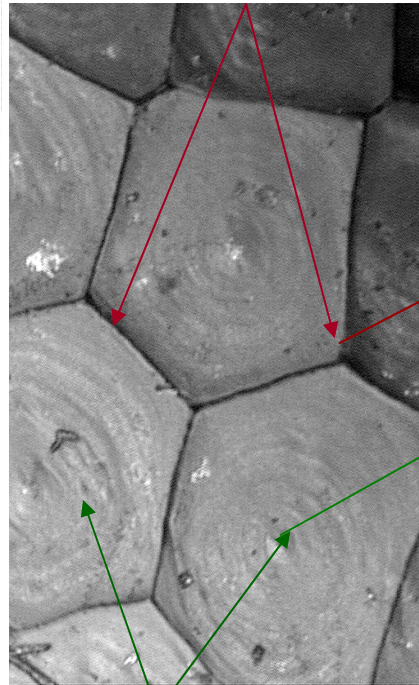
Small glassy inclusions in volcanic olivine grains, with 900 – 1700 ppm Sulphur



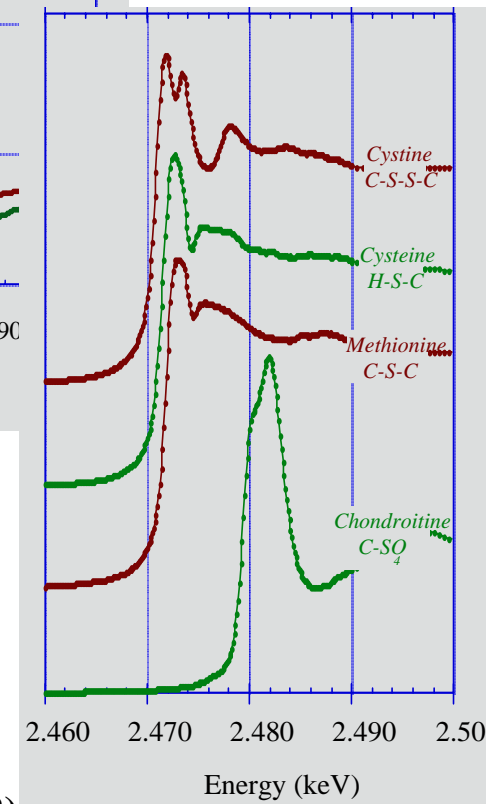
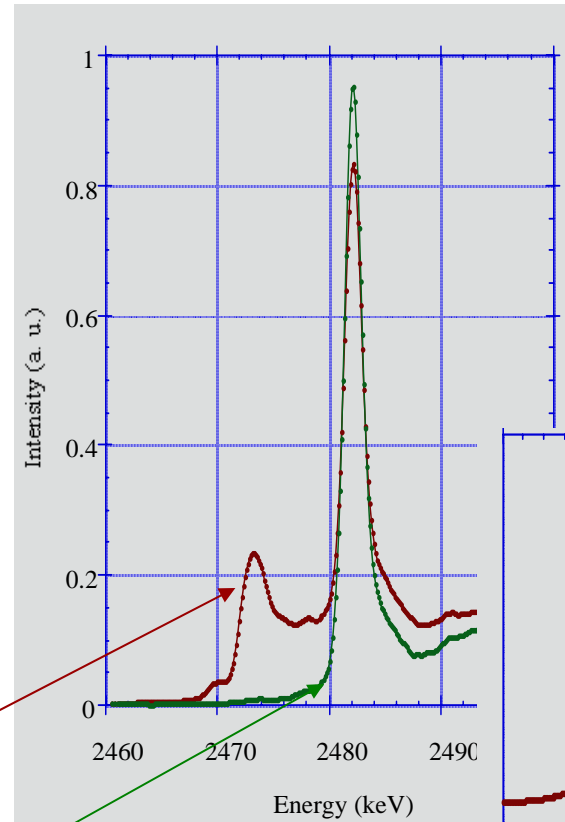
Sulfur K-edge in Pinna



Organic matrix



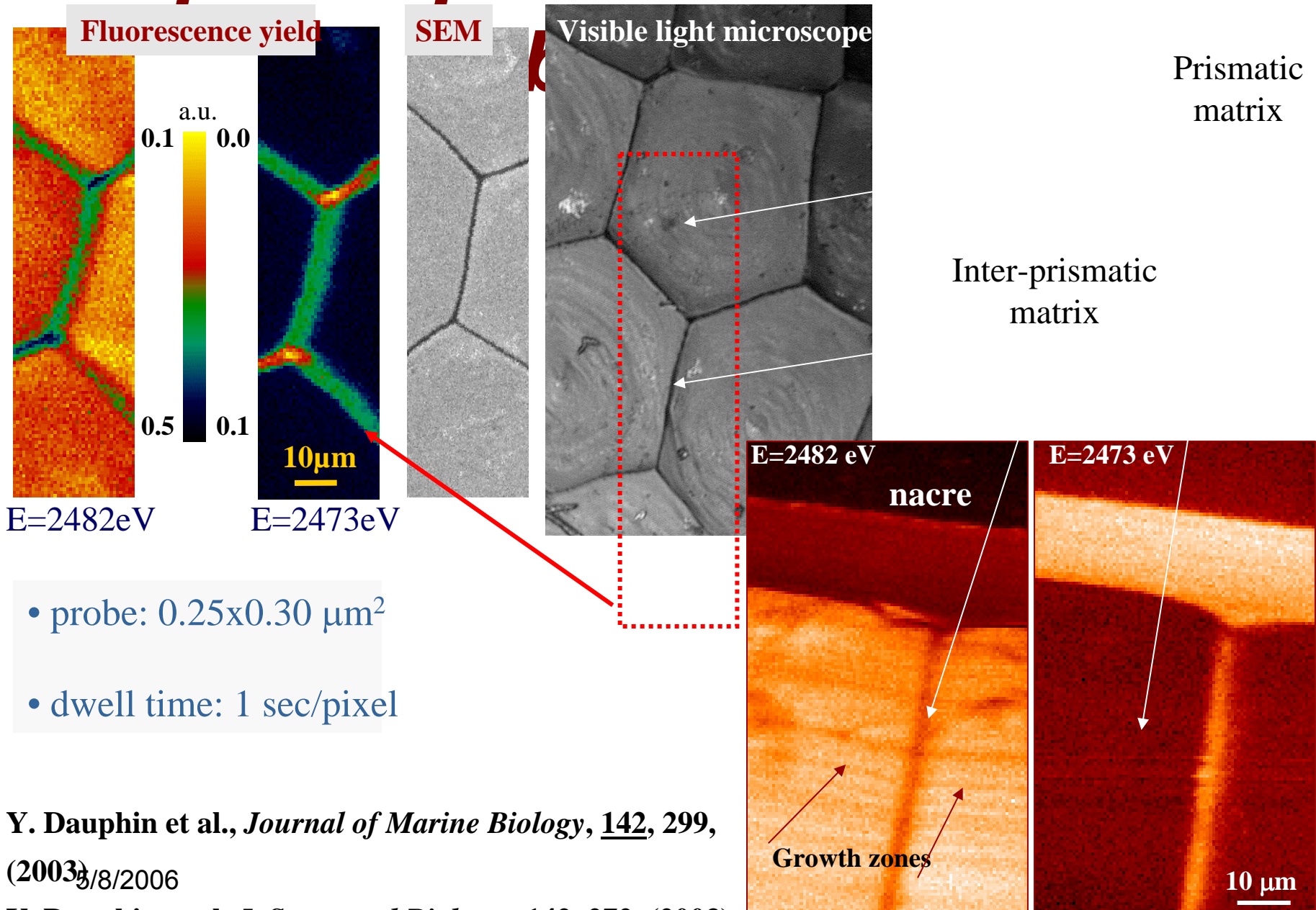
Mineral prisms



5/8/2006

Y. Dauphin et al., *Comparative Biochemistry and Physiology, Part A* **132**, (2002)

Sulphur species in Pinna

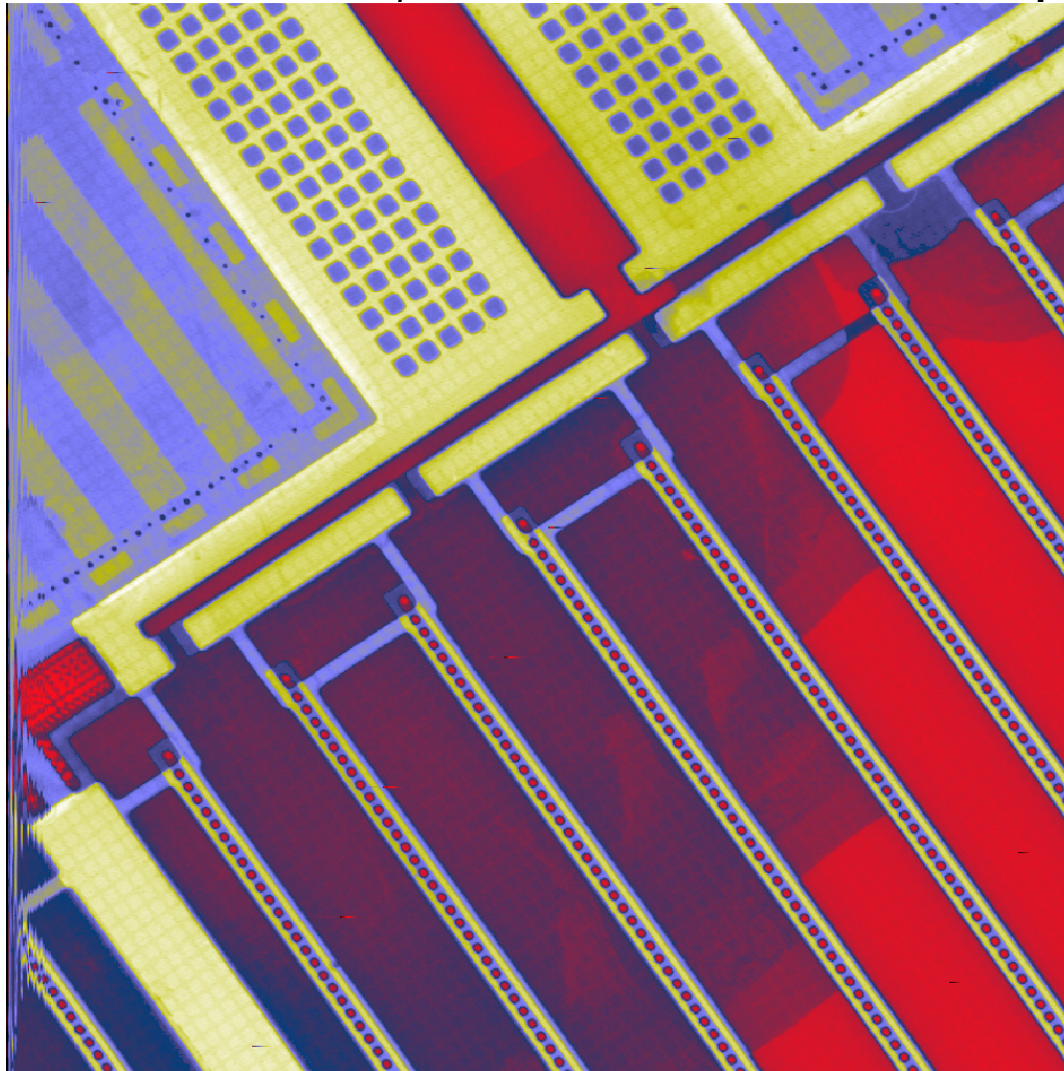


Y. Dauphin et al., *Journal of Marine Biology*, **142**, 299, (2003) 3/8/2006

Y. Dauphin et al. *J. Structural Biology*, **142**, 272, (2003)

STXM at APS

1830 eV; XRADIA 50 nm zone plate

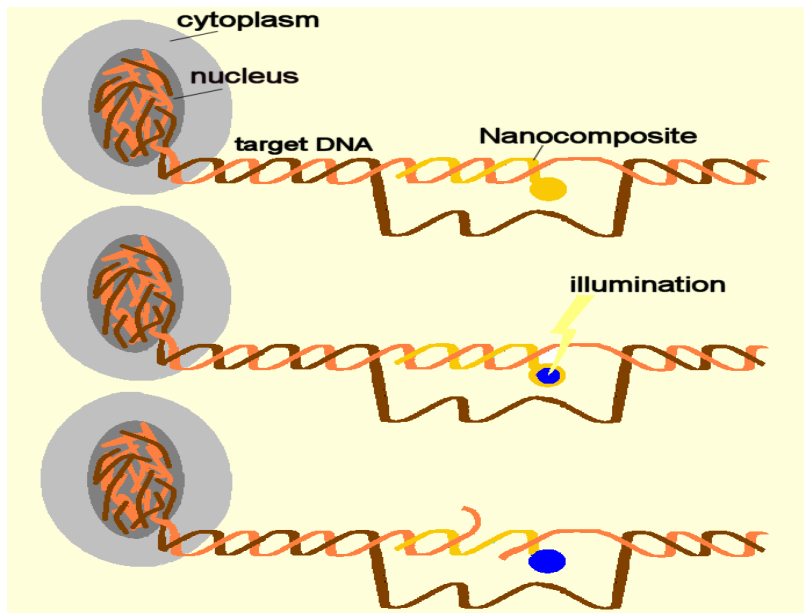


McNulty, 2002

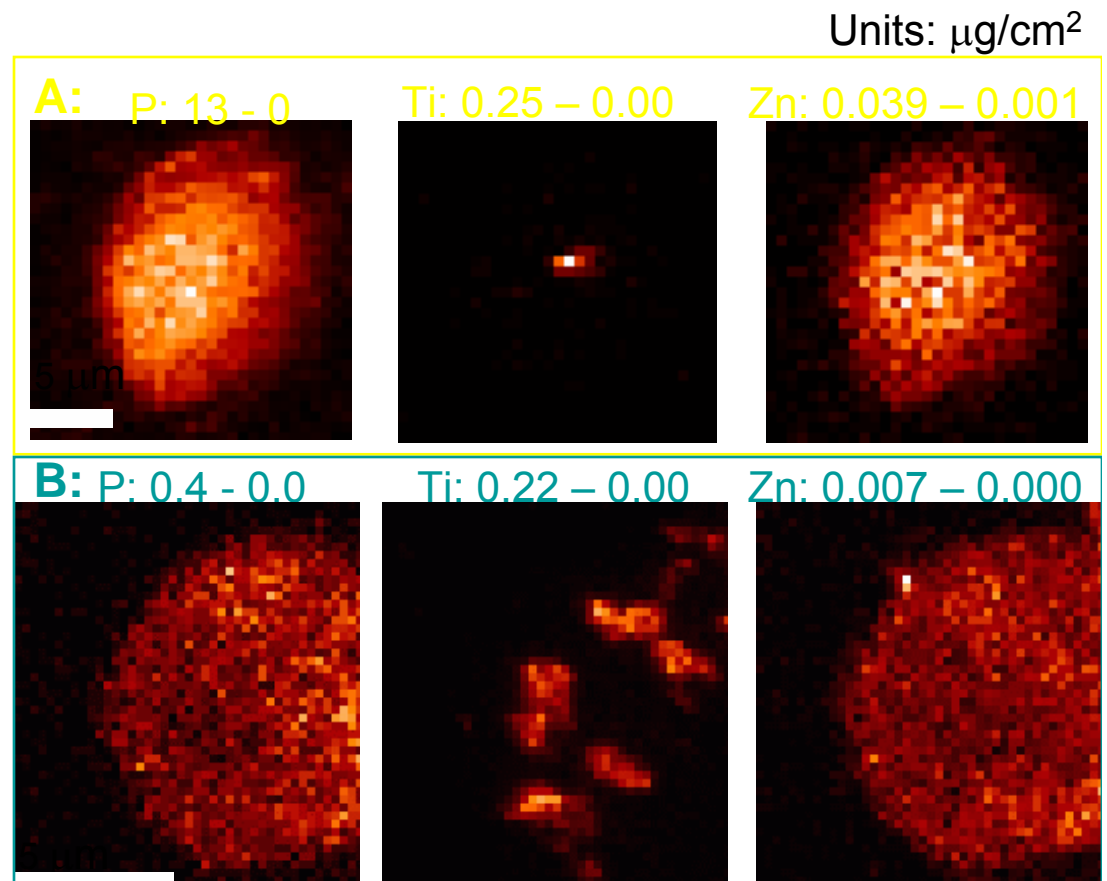
TiO₂-DNA nanocomposites as intracellular probes

- Cell is transfected with TiO₂-DNA nanocomposites (4.3 nm Ø)
- DNA is used to target nanocomposite to specific chromosomal region
- TiO₂ allows photocleavage of targeted DNA strand upon illumination
- potential to be used to for gene therapy

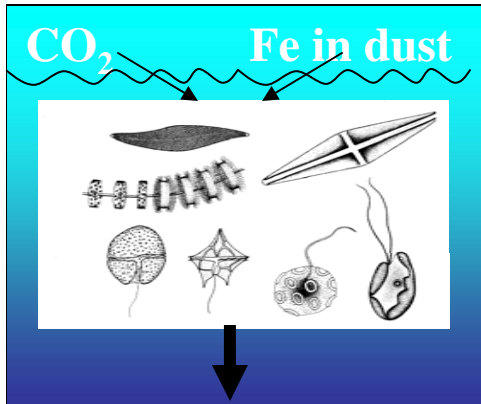
- map Ti distribution using X-ray induced K_α fluorescence, to quantify the success rate of TiO₂-DNA transfection, and visualize target
- **A:** scan of a MCF7 cell transfected with nanocomposites targeted to nucleolus
- **B:** scan of a PC12 cell transfected with nanocomposites targeted to mitochondria



5/8/2006
T. Paunescu *et al.*, Nature Materials 2,
343-346 (01. May 2003)

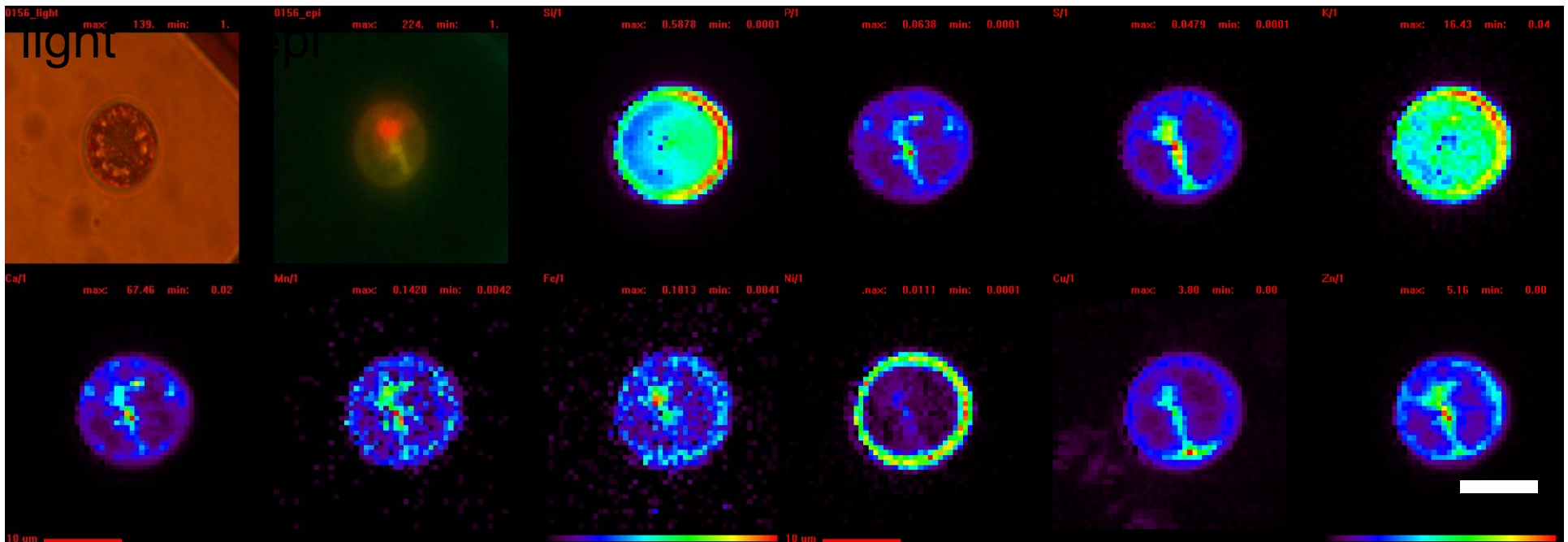


Trace metals in plancton and global carbon balance



- CO_2 sequestration in the ocean seems to be limited by the availability of Fe (necessary for Chlorophyll production).

CO_2 sequestration by Fe seeding



5/8/2006

B. Twining, *et al.*,
Analytical Chemistry 75, 3806-3816 (2003).

70

Why I like scanning?

- XANES spectroscopy
 - Multi-channel detector
 - Low dose, large area overview scans
 - Convenient correlation to visible light microscopy
 - Wet, dry, or cryo specimens
 - Minimizes radiation dose
 - Quantitative
-
- Relatively slow: pixel by pixel